ELSEVIER

Contents lists available at ScienceDirect

Science of the Total Environment

journal homepage: www.elsevier.com/locate/scitotenv





Prenatal exposure to dietary levels of glyphosate disrupts metabolic, immune, and behavioral markers across generations in mice

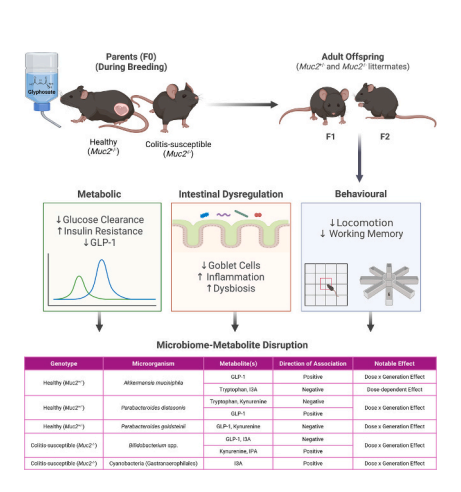
J.A. Barnett ^a, J.K. Josephson ^a, E. Yuzbashian ^a, N. Haskey ^a, M.M. Hart ^a, K.K. Soma ^{b,c,d}, A. Verdugo ^a, C.J. McComb ^a, M.L. Bandy ^a, S. Ghosh ^a, C. Letef ^a, A. Copp ^a, R. Ishida ^a, J. Gibon ^a, J. Ye ^a, R.T. Giebelhaus ^{e,f}, S.J. Murch ^e, M.M. Jung ^b, D.L. Gibson ^{a,g,*}

- ^a Department of Biology, University of British Columbia, Kelowna, V1V 1V7, Canada
- ^b Department of Zoology, University of British Columbia, Vancouver, V6T 1Z4, Canada
- ^c Djavad Mowafaghian Centre for Brain Health, University of British Columbia, Vancouver, V6T 1Z3, Canada
- ^d Department of Psychology, University of British Columbia, Vancouver, V6T 1Z4, Canada
- ^e Department of Chemistry, University of British Columbia; Kelowna, V1V 1V7, Canada
- f Department of Chemistry, University of Alberta, Edmonton, T6G 2N4, Canada
- ⁸ Faculty of Medicine, University of British Columbia, Kelowna, V1V 1V7, Canada

HIGHLIGHTS

- Prenatal glyphosate reshapes gut, metabolism and behaviour across multiple mouse generations.
- Harmful effects arise at 0.01mg/kg/day, a dose far beneath current safety limits.
- Gut barrier damage, mucin loss and inflammation persist into the F2 generation.
- Glyphosate-linked microbiome shifts disrupt endocrine and tryptophan pathways.
- Dose- and generation-based hostmicrobe rewiring suggests heritable gutbrain-immune disruption.

G R A P H I C A L A B S T R A C T



ARTICLE INFO

Keywords:
Glyphosate
Prenatal exposure
Gut microbiota
Gut barrier dysfunction
Transgenerational effects
Metabolic disruption

ABSTRACT

Glyphosate, a widely used herbicide in North America, has become prevalent in the food supply, raising concerns about potential health impacts. In this exploratory study, male and female F0 mice were exposed to glyphosate through drinking water during mating and gestation. We investigated whether prenatal exposure at dietary-relevant levels (0.01 mg/kg/day, Average American Diet, [AAD]) or the U.S. EPA's acceptable daily intake (1.75 mg/kg/day, [EPA Upper Limit]) altered gut, metabolic, and behavioral outcomes across two generations in mice with or without genetic susceptibility to colitis ($Muc2^{+/-}$ and $Muc2^{-/-}$, respectively). Healthy ($Muc2^{+/-}$) offspring of glyphosate-exposed mice exhibited colonic goblet cell depletion, reduced mucin-2 expression, and

https://doi.org/10.1016/j.scitotenv.2025.180437

Received 6 June 2025; Received in revised form 3 August 2025; Accepted 4 September 2025 Available online 25 September 2025

0048-9697/© 2025 The Authors. Published by Elsevier B.V. This is an open access article under the CC BY-NC license (http://creativecommons.org/licenses/by-nc/4.0/).

^{*} Corresponding author at: Department of Biology, University of British Columbia, Kelowna, V1V 1V7, Canada. *E-mail address*: Deanna.Gibson@ubc.ca (D.L. Gibson).

pro-inflammatory cytokine profiles in both F1 and F2 generations. These healthy $(Muc2^{+/-})$ offspring also developed metabolic dysfunction, including impaired glucose tolerance, insulin resistance, and reduced GLP-1 in serum. Behavioral deficits were also observed in healthy $(Muc2^{+/-})$ mice including reduced locomotion and working memory. These changes were accompanied by significant shifts in gut microbiome composition and associations between specific microbes, including Akkermansia muciniphila and Parabacteroides distasonis and gutbrain signaling molecules including GLP-1 and serotonin, suggesting a microbiota-mediated mechanism for neuroendocrine disruption. In contrast, colitis-susceptible $(Muc2^{-/-})$ mice showed fewer overt exposure effects, likely due to masking by their baseline disease phenotype, but did show alterations consistent with enteric neuroinflammation resulting from glyphosate exposure including blooms in Cyanobacteria and reduced tryptophan metabolites. These findings suggest that prenatal glyphosate exposure, even below regulatory thresholds, may disrupt multiple physiological systems across generations, highlighting the need for further research and potential regulatory consideration.

1. Introduction

Glyphosate (Roundup®) is one of North America's most widely used herbicides, with over 160 million kilograms applied annually (Beckie et al., 2020; A Survey on the Uses of Glyphosate in European Countries, n. d.). Agricultural practices, including the development of glyphosateresistant crops and glyphosate's use as a pre-harvest desiccant, have led to increased residues in commonly consumed foods such as wheat, corn, soy, and oats (Canadian Food Inspection Agency, 2017). These ingredients form the basis of the Western diet, which is frequently linked to chronic inflammatory diseases, including Inflammatory Bowel Disease (IBD) (Clemente-Suárez et al., 2023; Kopp, 2019; Carrera-Bastos et al., 2011). While this association is typically attributed to the poor nutritional quality of the Western diet, far less attention has been paid to the environmental contaminants embedded within it, particularly pesticide residues like glyphosate. This raises the possibility that the health consequences of the Western diet may not arise solely from its nutrient composition, but also from chronic, low-level chemical exposures that accompany its consumption.

Glyphosate targets the Shikimate pathway, which is found in plants, fungi, and bacteria but is absent in mammals (Barnett and Gibson, 2020). This absence initially led to the assumption that glyphosate was biologically inert in humans. However, emerging evidence suggests that glyphosate may indirectly affect host physiology by altering the gut microbiota (Barnett and Gibson, 2020; Barnett et al., 2022), modulating immune responses (Peillex and Pelletier, 2020), and disrupting endocrine signaling (Feng et al., 2025). These concerns are amplified during prenatal and early-life exposures when developmental systems are particularly sensitive to environmental cues. In addition to vertical transmission of microbes from mother to infant through delivery and breastfeeding, changes in maternal immunity, hormonal signaling, and microbiota-derived metabolites can shape fetal development through placental and lactational transfer, increasing the long-term risk for metabolic (Mulligan and Friedman, 2017), immune (Mirpuri, 2021), and neurodevelopmental disorders (Vuong et al., 2020; Sun et al.,

Most studies investigating glyphosate's biological effects rely on doses far exceeding those encountered through diet, limiting their realworld applicability (Barnett and Gibson, 2020; Barnett et al., 2022). Additionally, prior work has largely focused on direct exposure in healthy subjects, with little attention given to vulnerable populations or the possibility of transgenerational effects. It remains unclear whether glyphosate levels comparable to those found in the food supply can impact offspring health, particularly in the context of genetic susceptibility to disease. To address this gap, we examined whether prenatal glyphosate exposure at human-relevant levels, 0.01 mg/kg/day, reflecting estimated dietary intake (Average American Diet, AAD), and 1.75 mg/kg/day, the U.S. EPA's acceptable daily intake (EPA Upper Limit), disrupts immune, metabolic, and neurobehavioral outcomes across two generations in both healthy ($Muc2^{+/-}$) and colitis-susceptible (Muc2^{-/-}) mice. Based on previous studies that link glyphosate to microbiome disruption, we hypothesized that prenatal exposure at these doses would alter microbial composition and function, leading to increased intestinal inflammation, metabolic dysfunction, and behavioral changes that persist across generations in both genotypes.

2. Results

2.1. Prenatal glyphosate exposure induces microscopic colitis in healthy $(Muc2^{+/-})$ offspring and promotes intestinal inflammation

To assess how prenatal glyphosate exposure affects intestinal pathology, we examined markers of morbidity and inflammation in F1 and F2 offspring from healthy ($Muc2^{+/-}$) and colitis-susceptible ($Muc2^{-/-}$) mice. Although glyphosate-exposed healthy offspring did not exhibit overt colitis, histopathological analysis revealed morphological changes across both generations and exposure levels, consistent with microscopic colitis (Fig. 1A). Goblet cell depletion and crypt hyperplasia were the primary drivers of pathology (Fig. 1B–C), with goblet cell loss accompanied by reduced mucin-2 expression in the colon (Fig. 1C), indicating compromised mucus barrier function often seen in IBD patients (Kang et al., 2022).

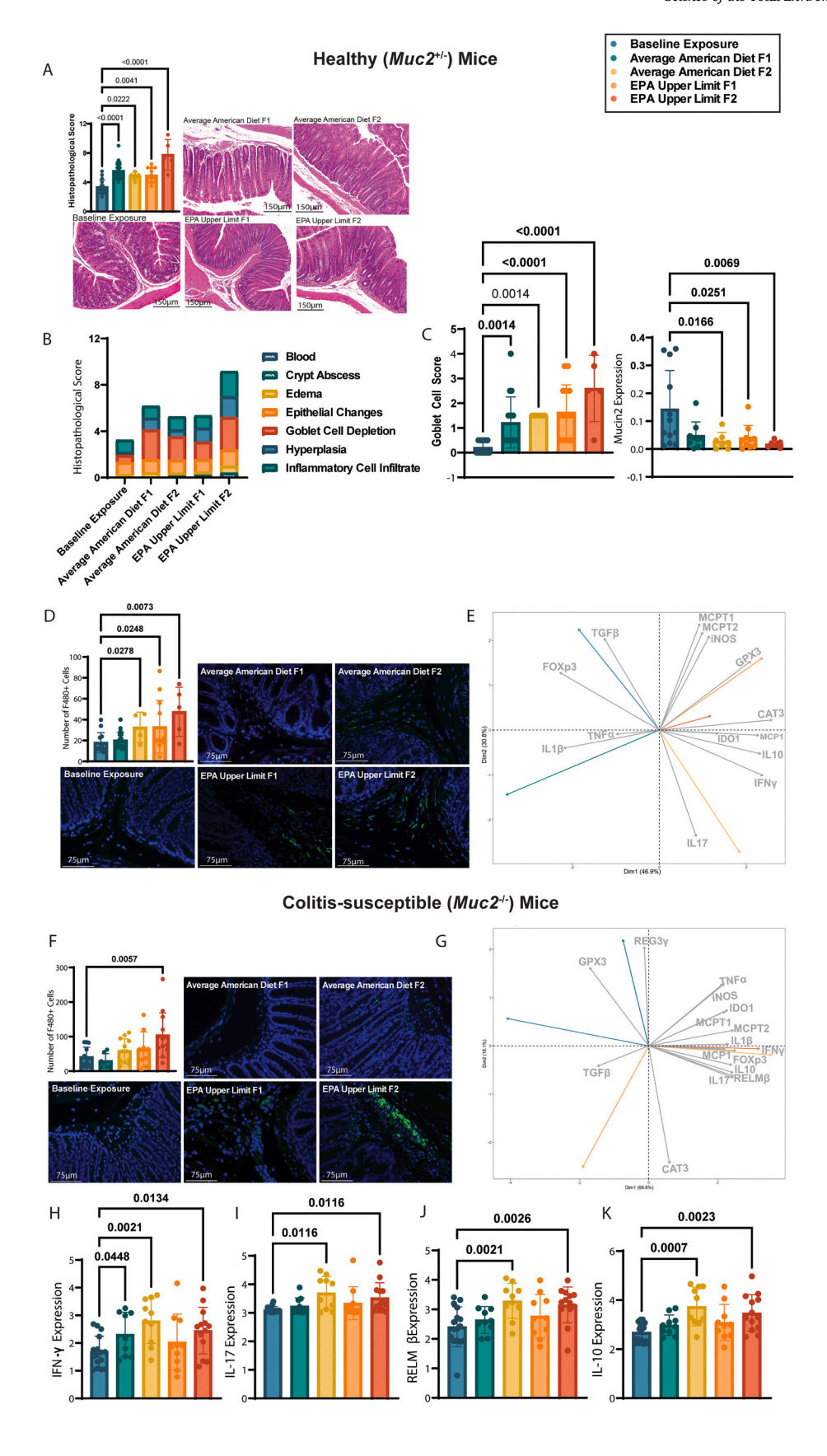
EPA F2 healthy ($Muc2^{+/-}$) offspring also showed increased F4/80+ macrophage infiltration in the colonic submucosa (Fig. 1D). Cytokine expression patterns, analyzed via Principal Component Analysis (PCA), showed distinct inflammatory signatures by treatment group (Fig. 1E) F1 offspring of AAD-exposed parents were characterized by a TNF-α and IL-1β–driven response, while F2 offspring shifted toward a Th17-like cytokine profile with enrichment in IFN- γ and IL-17. EPA-exposed groups showed upregulation of oxidative stress markers (GPX2, CAT3) and mast cell proteases (MCPT1, MCPT2), consistent with innate immune activation.

In colitis-susceptible ($Muc2^{-/-}$) offspring, prenatal glyphosate exposure had a more limited effect. EPA F2 mice showed elevated macrophage infiltration (Fig. 1F). PCA revealed a similar proinflammatory cytokine profile (Fig. 1G), including increased expression of IFN- γ , and IL-17 (Fig. 1H–K), but changes were modest compared to healthy ($Muc2^{+/-}$) littermates, potentially reflecting a ceiling effect due to baseline inflammation. Colitis-susceptible ($Muc2^{-/-}$) offspring also showed increased expression of the goblet cell mediator RELM- β , which has been shown to be a driving force in the development of colitis within this model (Morampudi et al., 2016).

These findings suggest that prenatal glyphosate exposure induces microscopic inflammation and mucus barrier dysfunction in healthy $(Muc2^{+/-})$ offspring, with effects that persist across generations. In colitis-susceptible $(Muc2^{-/-})$ mice, baseline inflammation may mask additional glyphosate-driven pathology.

2.2. Prenatal glyphosate exposure impairs glucose metabolism, reduces insulin sensitivity, and alters metabolic hormone production in healthy mice, with potential links to endotoxemia

Given the increased risk of metabolic syndrome in individuals with IBD (Shen et al., 2024), we next assessed whether prenatal glyphosate



(caption on next page)

Fig. 1. Prenatal glyphosate exposure induces microscopic colitis and colonic inflammation across generations in mice. (A) Histopathological scoring of colon tissue reveals increased damage in healthy (Muc2^{+/-}) F1 and F2 offspring of glyphosate-exposed parents compared to non-exposed animals. Damage was scored across crypt architecture, goblet cell abundance, and immune cell infiltration (Kruskal-Wallis, p < 0.0001, $\eta^2 = 0.493$, FDR-corrected; n = 5–16 per group). (B–C) Goblet cell depletion and epithelial hyperplasia were the primary contributors to histological scores (Two-way ANOVA, p = 0.0001, FDR-corrected). These changes were associated with decreased mucin-2 expression in colon tissue (Kruskal-Wallis, p=0.025, $\eta^2=0.178$). (D) Increased macrophage (F4/80+) infiltration was observed in the colonic submucosa of EPA F2 healthy ($Muc2^{+/-}$) offspring (Kruskal-Wallis, p = 0.015, $\eta^2 = 0.135$). (E) Principal component analysis (PCA) of colonic cytokine expression shows a pro-inflammatory shift in F1 and F2 glyphosate-exposed offspring, including enrichment of Th1/Th17 cytokines (e.g., TNF-α, IL-17, IFN-γ). (F–K) In colitis-susceptible ($Muc2^{-/-}$) offspring, glyphosate exposure induced modest increases in colonic inflammation, including elevated macrophage infiltration and increased expression of IFN- γ , IL-17, IL-10, and RELM- β (ANOVA/Kruskal-Wallis, FDR-corrected). Group Definitions: Baseline exposure = no glyphosate exposure in FO above that found within standard laboratory chow; AAD = Average American Diet intake level (0.01 mg/kg/day); EPA Upper Limit = U.S. EPA acceptable daily intake (1.75 mg/kg/day). "F1" and "F2" refer to first- and second-generation offspring of F0-exposed breeders. Genotypes: Muc2^{+/-} = healthy mice; Muc2^{-/-} colitis-susceptible mice. Sex: Sex was not found to be a driving factor in histopathological damage (PERMANOVA, p=0.268), goblet-cell depletion (PERMANOVA, p=0.268), goblet-cell depletion (PERMANOVA, p=0.268), goblet-cell depletion (PERMANOVA). = 0.485) or macrophage infiltration (PERMANOVA, p = 0.330) in healthy mice, however sex was found to influence mucin-2 gene expression (PERMANOVA, p = 0.019. In colitis-susceptible mice, sex was not found to be a driving factor in macrophage infiltration (PERMANOVA, p = 0.564), IFN-γ (PERMANOVA, p = 0.604), RELM- β (PERMANOVA, p=0.395), IL-17 (PERMANOVA, p=0.490), or IL-10 (PERMANOVA, p=0.765) gene expression. Primer sequences used for cytokine analysis are found in Table S5. Statistical Summary: Confidence intervals and sample sizes broken down by sex provided in Table S6.

exposure disrupted metabolic regulation in healthy (Muc2^{+/-}) and colitis-susceptible ($Muc2^{-/-}$) offspring. In the oral glucose tolerance test (OGTT), EPA-exposed healthy (Muc2^{+/-}) F2 offspring showed impaired glucose clearance, with elevated blood glucose 15 min post-gavage and increased AUC (Kruskal-Wallis, p = 0.0106, $\eta^2 = 0.129$; Fig. 2A). No such impairment was observed in the AAD group, suggesting a possible threshold effect for glyphosate-induced glycemic disruption in the F2 generation. In the insulin tolerance test (ITT), EPA-exposed F1 healthy $(Muc2^{+/-})$ mice showed reduced insulin sensitivity relative to nonexposed mice (ANOVA, p = 0.0326, $\eta^2 p = 0.174$; Fig. 2B). Serum GLP-1 levels were significantly reduced in both AAD- and EPA-exposed F1 and F2 offspring, with a trend toward reduction in AAD F2 mice (Kruskal-Wallis, p = 0.015, $\eta^2 = 0.145$; Fig. 2C). Ghrelin levels were lower in F1 mice, while leptin was elevated in AAD F1/F2 and EPA F1 offspring (Fig. 2D-E), suggesting dysregulated appetite control and possible leptin resistance (Nass et al., 2010; Tsai, 2017). This hormonal profile mirrors patterns observed in diet-induced obesity (Stępniowska et al., 2022) and gut permeability models (Wu et al., 2009; Ishioh et al.,

To explore whether these metabolic changes were linked to gut barrier dysfunction, we measured markers of endotoxemia and tight junction integrity. Serum LIX (CXCL5) levels were elevated in healthy ($Muc2^{+/-}$) offspring of glyphosate-exposed mice (Fig. 2F), consistent with systemic immune activation. In the colon, disorganized ZO-2 protein expression was observed in EPA F2 mice, suggesting tight junction disruption (Fig. 2G). These findings indicate compromised barrier function as a potential upstream driver of metabolic dysregulation. Similar to what was observed in intestinal pathology, colitis-susceptible ($Muc2^{-/-}$) offspring showed no glyphosate-related changes in glucose tolerance, insulin sensitivity, or hormone levels, again supporting a potential ceiling effect, where underlying inflammation and metabolic stress within the model eclipse additional glyphosate effects.

Together, these findings show that prenatal glyphosate exposure, at doses reflective of human dietary intake, disrupts metabolic regulation in healthy $(Muc2^{+/-})$ mice across generations. These effects likely arise through gut-mediated mechanisms involving barrier dysfunction and immune activation and appear less pronounced in mice with a preexisting susceptibility to intestinal inflammation $(Muc2^{-/-}$ mice).

2.3. Prenatal glyphosate exposure reduces locomotor activity, impairs working memory and alters the gut-brain axis in offspring

Individuals with IBD face an elevated risk of psychological and cognitive dysfunction (Hopkins et al., 2021; Nyuyki et al., 2018; Dadlani et al., 2021). To investigate whether glyphosate contributes to these outcomes across generations, we assessed behavior and gut-brain signaling in offspring following prenatal exposure. Glyphosate-exposed healthy ($Muc2^{+/-}$) offspring exhibited reduced locomotor activity, impaired working memory, and altered neuroimmune markers,

particularly in the F2 generation. In contrast, colitis-susceptible (*Muc2*^{-/}) offspring showed no overt behavioral changes but did exhibit molecular signatures of enteric neuroinflammation.

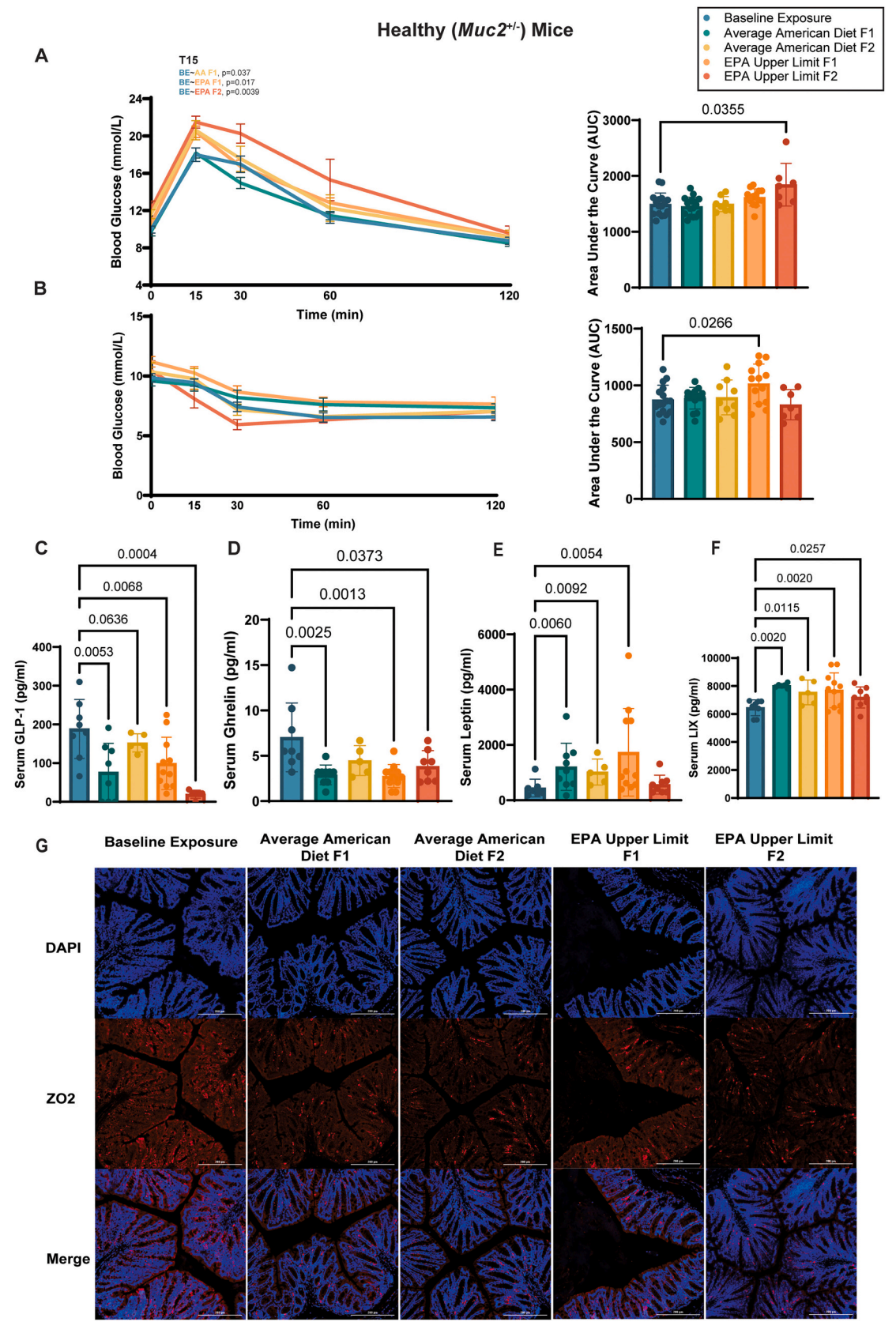
In the open field test, F2 EPA-exposed $Muc2^{+/-}$ mice travelled less distance and had lower average body velocity (p=0.0003, $\eta^2p=0.460$; Fig. 3A), indicating reduced locomotor activity. These mice also showed fewer unsupported rearings (p=0.018, $\eta^2p=0.219$; Fig. 3B), which may reflect diminished exploratory drive or subtle motor deficits. Anxiety-like behavior remained unchanged across exposure groups, based on center zone time, light/dark box preference, and serum corticosterone (Fig. S3). Working memory was impaired in F1 AAD-exposed $Muc2^{+/-}$ mice, which made more errors in the radial arm maze (p=0.041, $\eta^2p=0.147$; Fig. 3C). These deficits coincided with reduced serum kynurenine levels in both AAD F1 and EPA F2 offspring (p=0.024, $\eta^2=0.182$; Fig. 3D). Given kynurenine's role in generating neuroactive metabolites, this may signal disrupted neuroprotective metabolism.

While colitis-susceptible ($Muc2^{-/-}$) offspring did not show behavioral impairments, F2 AAD and EPA groups exhibited increased colonic expression of α -synuclein, GFAP, and SNAP-25 (p < 0.05, FDR-corrected; Fig. 3E), consistent with enteric neuroinflammation and early neurodegenerative signaling. EPA F2 $Muc2^{-/-}$ mice also had lower serum serotonin (p = 0.031, $\eta^2 = 0.188$; Fig. 3F), a key neurotransmitter involved in gut-brain signaling and motility. Although behavioral phenotypes were restricted to healthy offspring, the gut-brain molecular changes observed in colitis-susceptible mice suggest latent neurophysiological disruption. Together, these findings show that prenatal glyphosate exposure, at or below levels deemed safe, can affect neurodevelopment and behavior through gut-brain axis pathways.

2.4. Prenatal glyphosate exposure alters gut bacteriome composition, microbial metabolism, and predicted functional potential in offspring

Community level structure was not significantly altered when assessed using alpha- and beta-diversity metrics. Furthermore, no MetaCyc or KEGG pathways reached statistical significance (FDR < 0.05) in any exposure group or generation. However, prenatal glyphosate exposure induced taxonomic shifts in both healthy ($Muc2^{+/-}$) and colitis-susceptible ($Muc2^{-/-}$) offspring across generations, with genotype-specific patterns emerging (Fig. 4). In healthy offspring, Akkermansia muciniphila was more abundant in baseline controls (Fig. 4A). Given its role in supporting barrier integrity and regulating GLP-1 (Cani and Knauf, 2021) and NF-kB signaling (Shi et al., 2022), its depletion in exposed groups may underlie both metabolic and inflammatory phenotypes.

In contrast, *Parabacteroides distasonis* and *P. goldsteinii* were elevated in AAD F2 mice. While sometimes considered beneficial, *P. distasonis* has been linked to depression-like behavior in murine colitis models, pointing to context-dependent effects on host physiology (Taglialegna,



(caption on next page)

Fig. 2. Prenatal glyphosate exposure impairs glucose regulation and alters metabolic hormones in healthy $(Muc2^{+/-})$ offspring across generations. (A) Oral glucose tolerance test (OGTT) in F2 offspring reveals impaired glucose clearance in EPA-exposed healthy $(Muc2^{+/-})$ mice compared to non-exposed controls (Kruskal-Wallis, p=0.0106, $\eta^2=0.129$, FDR-corrected; n=10-12 per group). (B) Insulin tolerance test (ITT) in F1 healthy $(Muc2^{+/-})$ offspring shows reduced insulin sensitivity in the EPA group (ANOVA, p=0.0326, $\eta^2p=0.174$, FDR-corrected). (C) GLP-1 levels were significantly reduced in both AAD- and EPA-exposed F1 and F2 $Muc2^{+/-}$ mice (Kruskal-Wallis, p=0.015, $\eta^2=0.145$, FDR-corrected). (D) Ghrelin levels were decreased in F1 healthy $(Muc2^{+/-})$ offspring following prenatal glyphosate exposure. (E) Leptin levels were elevated in AAD F1/F2 and EPA F1 offspring, suggesting potential leptin resistance. (F) Serum levels of LIX (CXCL5), a neutrophil chemoattractant linked to intestinal permeability and inflammation, were elevated in glyphosate-exposed offspring. (G) Immunofluorescent staining for ZO-2 revealed disrupted tight junction organization in the colonic epithelium of EPA F2 mice, indicative of barrier dysfunction. **Group Definitions:** Baseline exposure = no glyphosate exposure in F0 above that found within standard laboratory chow; AAD = Average American Diet intake level (0.01 mg/kg/day); EPA Upper Limit = U.S. EPA acceptable daily intake (1.75 mg/kg/day). "F1" and "F2" refer to first- and second-generation offspring of F0-exposed breeders. **Genotypes:** $Muc2^{+/-}$ = healthy mice; $Muc2^{-/-}$ = colitis-susceptible mice (not shown). **Sex:** Sex was found to influence glucose tolerance (PERMANOVA, p=0.042), and may influence insulin tolerance (PERMANOVA, p=0.042), and may influence in the observed changes in serum GLP-1 (PERMANOVA, p=0.062). Sex was not found to be a driving influence in the observed changes in serum GLP-1 (PERMANOVA, p=0.062). Sex was not found to

2024). EPA F2 mice also showed increased Christensenellaceae, a highly heritable taxon associated with gut-brain signaling and Parkinson's disease risk (Romano et al., 2021; Waters and Ley, 2019). These changes suggest glyphosate exposure shifts the microbial ecosystem toward profiles linked to metabolic and neurological vulnerability. Cecal metabolite analysis revealed elevated acetate in AAD F1 mice (Fig. 4B) While short-chain fatty acids are typically beneficial, excess acetate has been associated with parasympathetic overactivation and features of metabolic syndrome, suggesting a potential mechanism by which even low-dose glyphosate might disrupt host energy balance (Perry et al., 2016).

In colitis-susceptible ($Muc2^{-/-}$) offspring, *Bifidobacterium* spp. were increased in EPA F1 mice (Fig. 5C). Although typically regarded as beneficial, elevated Bifidobacterium spp. have been reported during active IBD flares, suggesting its expansion may reflect intestinal inflammation (Wang et al., 2014). Additionally, colitis-susceptible $(Muc2^{-/-})$ F2 offspring within the EPA Upper Limit group exhibited an increased abundance of non-photosynthetic cyanobacteria, specifically Gastranaerophilales. In the environment, glyphosate promotes the growth of cyanobacteria as it provides a rich source of phosphorus needed for these organisms to thrive (Drzyzga and Lipok, 2018). However, this study is the first to demonstrate that dietary glyphosate can promote the growth of cyanobacteria in the gut. Functional profiling using BugBase (Ward et al., 2017) showed colitis-susceptible offspring in the EPA group harbored a microbiome enriched with aerobic, pathogenic, and biofilm-forming taxa across both F1 and F2 generations (Fig. 4D). These features are consistent with microbial dysbiosis and may exacerbate barrier disruption and immune activation. Given that glyphosate targets the EPSPS enzyme in the Shikimate pathway, and that most commensals possess Class I EPSPS enzymes (glyphosate-sensitive), while several pathogens carry resistant Class II variants, these shifts likely reflect a selective pressure favoring glyphosate-tolerant taxa (Barnett and Gibson, 2020; Barnett et al., 2022). These results show that while the gut microbiome remains largely stable, prenatal glyphosate exposure reconfigures it in ways that may promote inflammation, metabolic dysfunction, and neuroimmune disruption. The persistence of these shifts across generations and their emergence at human-relevant doses highlights their potential significance for long-term health.

2.5. Prenatal glyphosate exposure impacts microbe-metabolite interactions in a dose and generation dependent manner

Given the observed shifts in bacterial taxa with known metabolic and inflammatory roles, we performed a correlational analysis to determine whether glyphosate-induced changes in microbial composition were associated with altered metabolite levels. Because several microbial derivatives of tryptophan, including the indole metabolites indole-3-aldehyde (I3A) and 3-indolepropionic acid (IPA), play key roles in ost immune and metabolic signaling, these were included alongside canonical host metabolites in the analysis. Notably, *Akkermansia muciniphila* abundance was positively correlated with GLP-1 levels ($\rho = 0.428$,

p=0.011), whereas *Parabacteroides distasonis* showed a significant negative correlation with GLP-1 (Fig. 5A & B, $\rho=-0.42$, p=0.0127). These associations remained significant after adjusting for glyphosate exposure (dose effect p<0.05; microbe \times group interaction p>0.1), indicating a consistent relationship across baseline-exposure, AAD and EPA exposure levels. In addition to GLP-1, *A. muciniphila* was inversely correlated with serum tryptophan levels ($\rho=-0.43$, p=0.011) and its microbial metabolite I3A ($\rho=-0.53$, p<0.001). *P. distasonis* also negatively correlated with tryptophan levels ($\rho=-0.42$, p=0.013). ANCOVA confirmed significant dose effects for tryptophan (p<0.05), with non-significant microbe \times group interactions, suggesting robust associations across exposure levels.

To assess whether these microbe-metabolite relationships varied by generation, we modeled three-way interactions (abundance \times dose \times generation). Significant dose \times generation effects emerged for GLP-1 in association with A. muciniphila (p=0.022), P. distasonis (p=0.002), P. goldsteinii (p=0.016) and for kynurenine with P. distasonis (p=0.0037) and P. goldsteinii (p=0.0200) (Fig. 5C). These findings suggest that ancestral glyphosate exposure influences the strength of microbehormone associations, particularly within the GLP-1 and kynurenine nathways

Dose-response analysis revealed a significant overall decline in GLP-1 with increasing glyphosate exposure (Fig. 5D, Jonckheere-Terpstra [JT] p=0.003), driven largely by F2 offspring (JT p=0.031). In contrast, microbial abundances of *A. muciniphila, P. distasonis*, and *P. goldsteinii* did not follow a clear monotonic pattern, indicating that GLP-1 suppression likely results from direct prenatal glyphosate exposure, with microbial contributions acting in an additive rather than exclusively mediating manner.

In colitis-susceptible ($Muc2^{-/-}$) mice, Bifidobacterium spp., abundance was not significantly correlated with serum levels of GLP-1, leptin, serotonin, kynurenine, IPA, or tryptophan. Although no significant microbe \times group interaction was observed, three-way interactions revealed significant dose \times generation effects for Bifidobacterium and GLP-1 (p=0.003), kynurenine (p=0.044), IPA (p=0.014) and I3A (p=0.013) (Fig. 5E & F). Cyanobacteria also showed a significant dose \times generation effect for I3A (p=0.013). While no consistent dose-response trends in metabolite levels were observed across all groups, stratified analyses revealed a positive trend for leptin in F1 (JT p=0.045) and a negative trend for serotonin in F2 (JT p=0.048), suggesting generation-specific effects of glyphosate exposure on offspring metabolic signaling. These results suggest that prenatal glyphosate exposure is associated with generation and dose-dependent shifts in host-microbe-metabolite relationships.

3. Discussion

The findings of this exploratory study show that prenatal glyphosate exposure, even at doses previously considered safe, induces measurable physiological changes in offspring across generations. In healthy $(Muc2^{+/-})$ mice, glyphosate exposure induced colonic histopathology

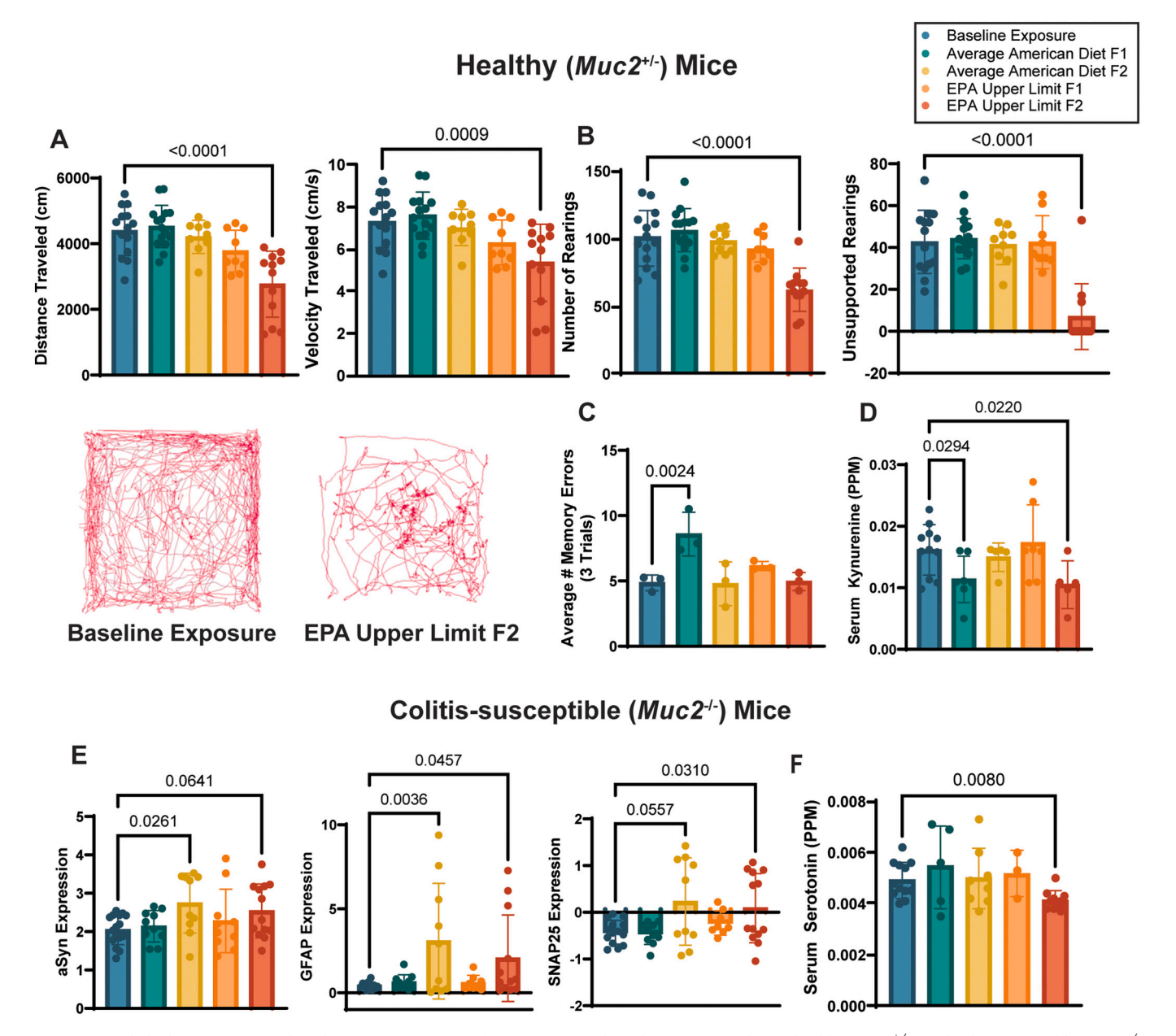
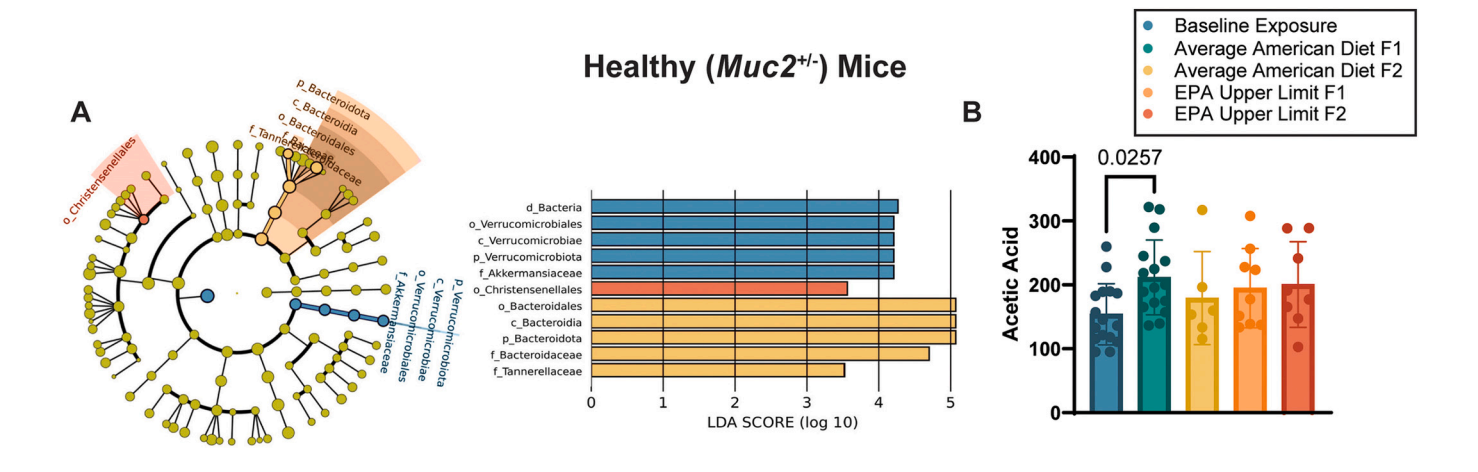


Fig. 3. Prenatal glyphosate exposure alters locomotor activity, working memory, and gut–brain axis signaling in healthy $(Muc2^{+/-})$ and colitis-susceptible $(Muc2^{-/-})$ offspring. (A) Healthy $(Muc2^{+/-})$ EPA F2 offspring exhibited significantly reduced distance travelled and body velocity in the open field test $(p=0.0003, \eta^2p=0.460, FDR$ -corrected; n=6-10/group). (B) Unsupported rearing frequency was significantly reduced in the same group $(p=0.018, \eta^2p=0.219)$, suggesting impaired exploratory behavior. (C) AAD F1 healthy $(Muc2^{+/-})$ offspring displayed impaired working memory, reflected by increased radial arm maze errors $(p=0.041, \eta^2p=0.147)$. (D) Serum kynurenine levels were significantly reduced in AAD F1 and EPA F2 healthy $(Muc2^{+/-})$ offspring $(p=0.024, \eta^2=0.182)$, consistent with disruption of neuroprotective metabolic pathways. (E) F2 colitis-susceptible $(Muc2^{-/-})$ offspring exhibited elevated expression of α-synuclein, GFAP, and SNAP-25 in colonic tissue following AAD and EPA exposure (all p<0.05, FDR-corrected), suggesting enteric neuroinflammation. (F) Serum serotonin was significantly reduced in EPA F2 $Muc2^{-/-}$ offspring $(p=0.031, \eta^2=0.188)$, a neurotransmitter involved in gut-brain signaling and motility. **Group Definitions:** Baseline exposure = no glyphosate exposure in F0 above that found within standard laboratory chow; AAD = Average American Diet intake level (0.01 mg/kg/day); EPA Upper Limit = U.S. EPA acceptable daily intake (1.75 mg/kg/day). "F1" and "F2" refer to first- and second-generation offspring of F0-exposed breeders. **Genotypes:** $Muc2^{+/-}$ = healthy mice; $Muc2^{-/-}$ = colitis-susceptible mice. **Sex:** Sex was not found to be a significant predictor for changes observed in distance (PERMANOVA, p=0.757,), velocity (PERMANOVA, p=0.792), total rearing events (PERMANOVA, p=0.346) in healthy mice. Sex was not found to be a significant predictor for changes observed in serum serotonin levels (PERMANOVA, p=0.662), α-synuclein (PERMANOV

marked by goblet cell depletion and epithelial hyperplasia. Loss of goblet cells reduced mucin-2 production and weakened the mucus barrier, potentially allowing microbial translocation and contributing to immune activation, as indicated by elevated serum LIX. These effects were absent in colitis-susceptible ($Muc2^{-/-}$) mice, suggesting that glyphosate primarily impacts barrier integrity in hosts with intact

immune and mucus signaling pathways.

Both genotypes showed a shift toward a pro-inflammatory Th1/Th17 cytokine profile. These findings contrast with asthma model studies where glyphosate suppressed IL-17 and IFN- γ , highlighting how cytokine responses may vary by tissue and context (Buchenauer et al., 2022). Glyphosate's known non-monotonic dose-response behavior may also



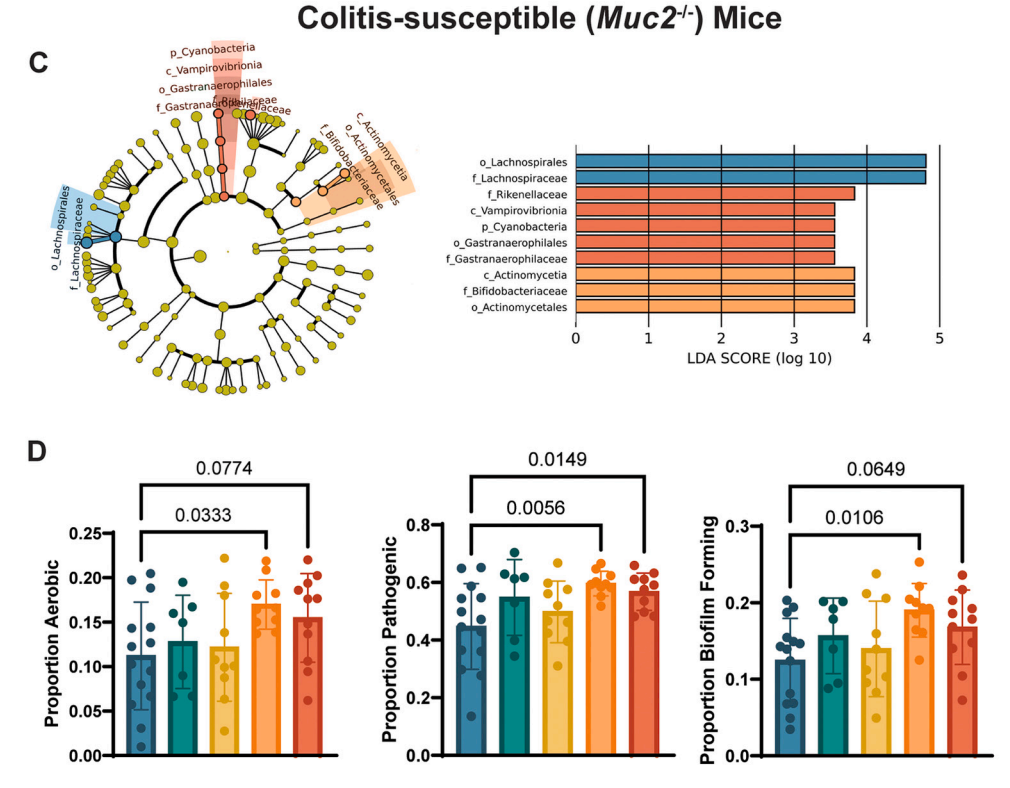


Fig. 4. Prenatal glyphosate exposure alters gut microbial composition, SCFA levels, and predicted microbial function across generations. (A) Microbial taxa affected by prenatal glyphosate exposure in healthy ($Muc2^{+/-}$) offspring included *Parabacteroides distasonis*, *P. goldsteinii*, and Christensenellaceae, all of which were significantly elevated in AAD or EPA F2 mice. Notably, *Akkermansia muciniphila* was more abundant in unexposed offspring, consistent with its role in maintaining gut barrier integrity and maintaining metabolic homeostasis. (B) Cecal acetate levels were significantly increased in AAD F1 offspring (p = 0.064, $η^2p = 0.144$), suggesting altered microbial fermentation and potential implications for host metabolic regulation. (C) In colitis-susceptible ($Muc2^{-/-}$) mice, glyphosate exposure was associated with enrichment of *Bifidobacterium* spp. (EPA F1) and Gastranaerophilales (EPA F2), including non-photosynthetic cyanobacteria suggesting a possible interaction between glyphosate and microbial phosphorus metabolism. (D) BugBase functional prediction revealed that $Muc2^{-/-}$ offspring exposed to EPA doses harbored microbiota with increased proportions of aerobic (p = 0.0676, $η^2p = 0.167$), biofilm-producing (p = 0.0365, $η^2p = 0.192$), and pathogenic bacteria (Welch's ANOVA, p = 0.0137, $ω^2 = 0.370$), consistent with a dysbiotic microbial community. **Group Definitions:** Baseline exposure = no glyphosate exposure in F0 above that found within standard laboratory chow; AAD = Average American Diet intake level (0.01 mg/kg/day); EPA Upper Limit = U.S. EPA acceptable daily intake (1.75 mg/kg/day). "F1" and "F2" refer to first- and second-generation offspring of F0-exposed breeders. **Genotypes:** $Muc2^{+/-}$ = healthy mice; $Muc2^{-/-}$ = colitis-susceptible mice. **Sex:** Sex was not found to be a significant predictor of acetic acid production in healthy mice (PERMANOVA, p = 0.739) nor any of the predicted functional analysis conducted in colitis-susceptible mice (PERMANO

contribute, where effects emerge at low or high doses but are not always linear (Hill et al., 2018). All animals received trace glyphosate from chow (~0.0015 mg/day), thus our baseline group represents low environmental exposure rather than true glyphosate-free conditions.

However, this exposure was 1–2 orders of magnitude lower than that of the exposed groups, and the additional waterborne exposure in AAD and EPA groups was enough to drive phenotypes, especially at the lower AAD dose. These findings support a threshold-based, non-monotonic

GLP-1

Ghrelir

Leptin

0.0140 0.0129

I3A

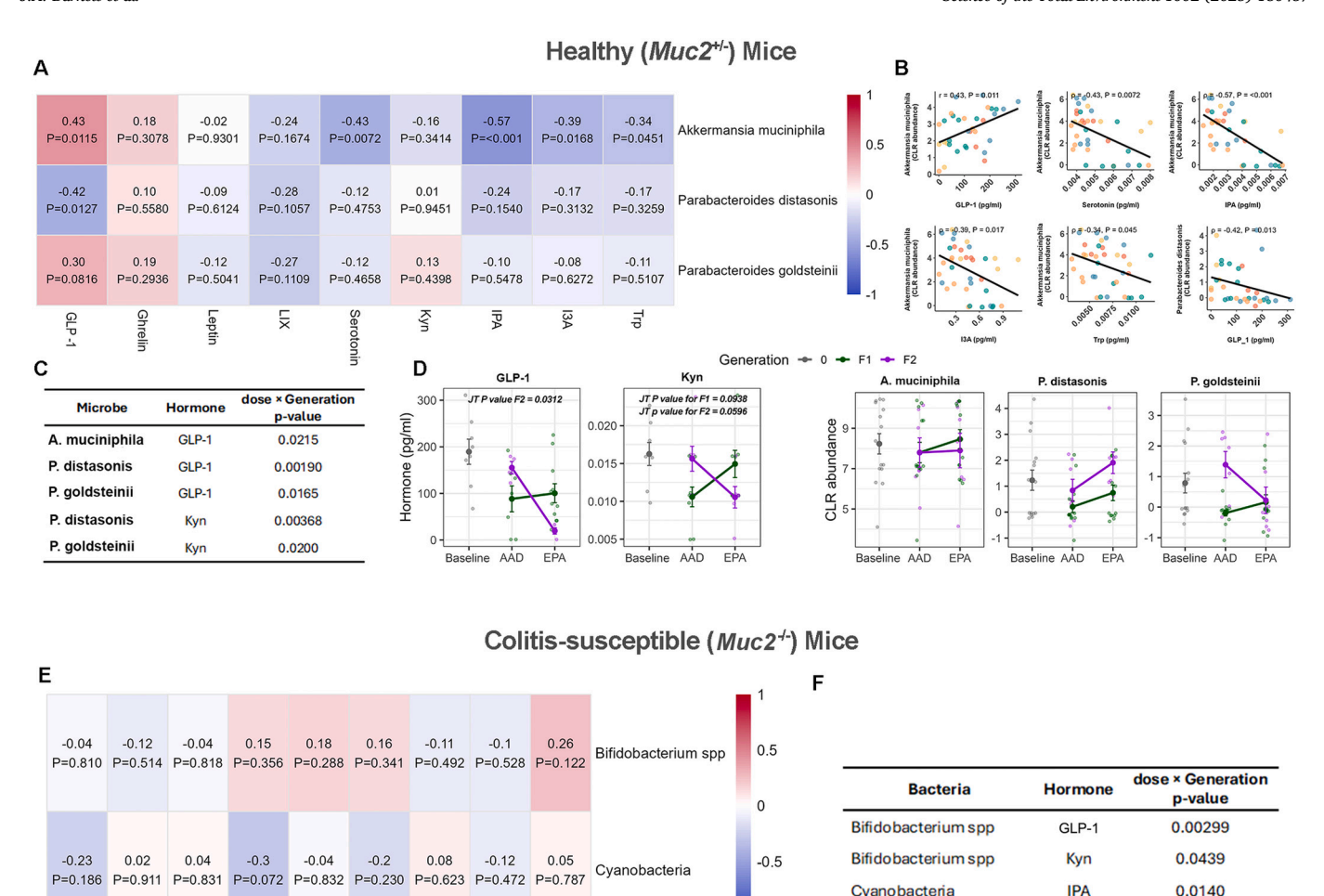


Fig. 5. Prenatal glyphosate exposure impacts microbe-metabolite associations. (A) Spearman correlation heatmap between centered log-ratio (CLR)-transformed abundances of Akkermansia muciniphila, Parabacteroides distasonis, and Parabacteroides goldsteinii and serum hormones (GLP-1, Ghrelin, Leptin, LIX, Serotonin) and tryptophan-derived metabolites (Kyn, IPA, I3A, Trp) in healthy (Muc2^{+/-}) mice. (B) Representative scatterplots for the significant correlations of microbe-metabolite pairs in healthy mice, showing CLR abundance versus serum concentration. (C) ANCOVA dose × generation interaction p-values for the five significant microbemetabolite associations in healthy mice. (D) Generation-stratified dose-response plots for GLP-1 and Kyn, with Jonckheere-Terpstra (JT) test p-values, and CLR abundance trajectories for A. muciniphila, P. distasonis, and P. goldsteinii. (E) Spearman correlation heatmap as in (A), but for Bifidobacterium spp. and nonphotosynthetic cyanobacteria in colitis-susceptible ($Muc2^{-/-}$) mice across the same exposure groups. (F) ANCOVA dose \times generation interaction p-values for significant microbe-metabolite/hormone associations in colitis-susceptible (Muc2^{-/-}) mice; ANCOVA models include main effects of abundance, dose, and generation, plus all interaction terms. All correlations are Spearman ρ (rho). ANCOVA models include main effects of abundance, dose, and generation, plus all interaction terms; only dose × generation p-values are shown. Jonckheere–Terpstra tests assess monotonic dose trends within each generation. **Group Definitions:** Baseline exposure = no glyphosate exposure in F0 above that found within standard laboratory chow; AAD = Average American Diet intake level (0.01 mg/kg/day); EPA Upper Limit = U.S. EPA acceptable daily intake (1.75 mg/kg/day). "F1" and "F2" refer to first- and second-generation offspring of F0-exposed breeders. Genotypes: Muc2^{+/} healthy mice; $Muc2^{-/-}$ = colitis-susceptible mice.

 \equiv

model of toxicity. Several effects, including working memory deficits and acetate accumulation, were observed in AAD but not EPA animals, underscoring the need to rethink dose-response assumptions for environmental exposures.

Kyn

IΡΑ

I3A

Тър

Metabolic disruption was evident in healthy (Muc2^{+/-}) AAD and EPA offspring, with reduced GLP-1 and altered leptin and ghrelin levels contributing to impaired glucose tolerance and insulin resistance. These findings align with CHAMACOS cohort data that link early-life glyphosate exposure to increased metabolic syndrome risk by age 18. Interestingly, later-life urinary glyphosate or AMPA levels were not predictive, reinforcing the concept that a specific developmental window of susceptibility exists for glyphosate's toxic effects (Eskenazi et al., 2023).

Behaviorally, healthy (Muc2+/-) EPA-exposed F2 mice showed reduced locomotor and exploratory activity and lower serum kynurenine, a precursor to neuroactive metabolites like kynurenic and quinolinic acid. An imbalance in this pathway can increase vulnerability to excitotoxicity and neuroinflammation, potentially contributing to observed behavioral impairments (Rahman et al., 2018). In contrast, colitis-susceptible ($Muc2^{-/-}$) offspring did not exhibit behavioral changes, likely due to the masking effects of their underlying colitis phenotype, which includes baseline behavioral and metabolic alterations that may mask subtle transgenerational effects. However, colitissusceptible (Muc2^{-/-}) mice did show signs of enteric neuroinflammation. SNAP-25, GFAP, and α-synuclein were highly expressed in AAD and EPA F2 groups, suggesting enteric neuronal stress and glial

Cvanobacteria

Cvanobacteria

activation (von Boyen et al., 2011; Liñán-Rico et al., 2016; Schaeffer et al., 2020). These changes are consistent with gut-brain signaling disruption and may represent early neurodegenerative processes, which have been observed following acute high-dose glyphosate exposure (Semchuk et al., 1992; Eriguchi et al., 2019; Bloem and Boonstra, 2023).

Microbiome shifts were observed across genotypes and generations. In healthy ($Muc2^{+/-}$) offspring, Akkermansia muciniphila was depleted, while Parabacteroides spp. and Christensenellaceae were enriched. Correlational analyses revealed that glyphosate exposure is associated with dose- and generation-dependent shifts in relationships between specific gut microbes and key metabolic and neuroactive metabolites, including GLP-1, tryptophan and their derivatives. Notably, taxa including Akkermansia muciniphila and Parabacteroides distasonis showed consistent associations with GLP-1 and tryptophan metabolism, suggesting that microbial composition may modulate host metabolic signaling following prenatal exposure. Although these findings are correlational, they support a model in which glyphosate disrupts the microbiome-host interface in a manner that may contribute to the observed behavioral and metabolic phenotypes across generations. The generation-specific patterns observed further underscore the potential for ancestral exposures to shape microbe-metabolite interactions and downstream host physiology. In particular, pertubations to microbial tryptophan metabolism, including production of immunomodulatory and neuroactive indole derivatives such as I3A and IPA, may represent a key link between glyphosate-induced community shifts and altered host signaling. In colitis-susceptible ($Muc2^{-/-}$) offspring, *Bifidobacterium* spp. was elevated in EPA F1 mice, similar to what is observed during active IBD in humans. Most striking was the increased abundance of Gastranaerophilales in EPA F2 mice. These cyanobacteria within the environment can produce the non-coding amino acid β-Methylamino-Lalanine (BMAA). BMAA can be incorporated into proteins where it acts as a neurotoxin through the misfolding of proteins and has been associated with neurodegenerative diseases like Parkinson's. It has been suggested that glyphosate runoff may contribute to algae blooms, increasing BMAA levels and contributing to the recent increase in neurological diseases observed in coastal areas across North America (Cecco, 2023; Koch, 2023). While enrichment of Cyanobacteria was noted in response to exposure to glyphosate, BMAA production was not measured here although it raises the possibility of gut-derived neurotoxic effects. Glyphosate's phosphonate group may select for microbes with enhanced phosphorus acquisition, offering one explanation for the emergence of this lineage. Importantly, Muc2^{+/-} and Muc2^{-/-} littermates were co-housed to minimize cage effects and standardize early microbial exposures. While co-housing enables microbial exchange, it reduces inter-cage variation and strengthens causal inference around treatment effects (Robertson et al., 2019). BugBase (Ward et al., 2017) profiling supported a shift toward dysbiosis in colitis-susceptible $(Muc2^{-/-})$ EPA offspring, with increased aerobic (Rigottier-Gois, 2013), pathogenic (Chow et al., 2011), and biofilm-forming (Muñiz Pedrogo et al., 2024; Palandurkar and Kumar, 2023) taxa, features associated with inflammation and barrier breakdown.

In this study, we cannot distinguish between germline (e.g., epigenetic) and microbiota-mediated mechanisms of transmission as we did not assess F0 breeders to avoid well reported stress-induced confounding effects. However, the appearance of phenotypes in the F2 generation is consistent with a transgenerational effect involving both host and microbial pathways. Future gnotobiotic experiments, including embryo transfer or microbiota transplantation, will be required to determine causal transmission mechanisms.

Given the limited statistical power of sex-stratified analyses within each treatment group, we employed PERMANOVA to assess interactions between sex and exposure across key outcomes. This multivariate non-parametric approach is well-suited to small and unbalanced group sizes and allowed us to examine the joint influence of sex and exposure

without overfitting. Significant sex \times exposure interactions were observed in mucin2 expression and microbial beta-diversity, indicating that some transgenerational effects may be modulated by sex-specific host-microbe interactions. While our study was not powered for comprehensive sex-stratified analyses, these findings highlight the importance of considering sex as a biological variable in future mechanistic work.

This study was designed as an exploratory, systems-level screening to identify potential domains of glyphosate-induced disruption. While mechanistic understanding was limited, the convergence of effects across behavioral, immune, and metabolic domains supports the need for further targeted investigation. Our findings demonstrate that prenatal glyphosate exposure, at doses consistent with real-world dietary intake, can disrupt multiple physiological systems across generations. Importantly, the emergence of effects at low doses suggests potential non-monotonic responses, which may obscure toxicity in traditional high dose testing paradigms. These results underscore the importance of reevaluating regulatory thresholds and prioritizing mechanistic studies, particularly those addressing critical development windows, microbiome-mediated effects, and transgenerational transmission, to fully assess the long-term health impacts of glyphosate exposure.

4. Materials and methods

4.1. Pre-registration

The original experimental design was pre-registered with the Open Science Framework (osf.io) on February 25th 2020. The pre-registration be viewed at osf.io/6nbsx. Changes made from original pre-registration can be found in Table S1.

4.2. Determination of the Average American Diet (AAD) dose

To determine the amount of glyphosate the average North American is exposed to through diet, we calculated the Average American Diet (AAD) dose based on a hypothetical menu for a 60 kg female following the American food guide and reported values of glyphosate found within these foods (Table 1). The AAD dose was determined to be 0.01 mg/kg/day, which is more than $100\times$ lower than the acceptable daily intake (ADI) currently set by the Environmental Protection Agency (EPA) at 1.75 mg/kg/day. At the time of dose calculation, few studies existed detailing glyphosate levels in food. Therefore, we relied on values collected from citizen science initiatives to calculate the AAD dose. To validate these reported levels of glyphosate in food, we developed a modified ultra-performance liquid chromatography method for quantification (Fig. S2). The values used to calculate the AAD dose were found to be similar to what has subsequently been reported in literature and our own measurements (Table 2).

We also assessed glyphosate content in the irradiated PicoLab® 5053 rodent chow used in this study. Tandem MS analysis revealed a glyphosate concentration of 0.381 μ g/g (381 ppb). Based on typical chow consumption (4–5 g/day) (University of North Carolina at Chapel Hill, 2021), this corresponds to a total glyphosate intake of approximately 0.00152–0.00191 mg/day per mouse. This background exposure was not adjusted for body weight and was consistent across all experimental groups, including unexposed controls. Therefore, animals in the AAD and EPA groups received this baseline amount plus their respective water-based doses of 0.01 mg/kg/day and 1.75 mg/kg/day, respectively. While glyphosate-free chow was not commercially available at the time of this study, this background exposure was minimal and equivalent across groups, allowing differences between AAD, EPA, and unexposed control animals to be attributed to the additional, controlled waterborne exposure.

Table 1 Calculation of the AAD dose. A hypothetical menu for an active female >20 years old (60 kg) following the American food guide.

Meal	Amount	Glyphosate Detected (ppb)	Total (µg/ serving)
Breakfast			
Cheerios	1 cup (27 g)	5775 (A Survey on the Uses of Glyphosate in European Countries, n.d.)	15.6
1 % Milk	1 cup	_	-
Apple, whole	1 medium	-	-
Snack	10 (00)		10.0
Ritz crackers	10 (32 g)	569 (Environmental Defence Canada, 2018)	18.2
Fontaine Sante roasted garlic hummus	1/4 cup (60 g)	760 (Environmental Defence Canada, 2018)	45.6
Water	No limit	-	-
Lunch			
PC Blue Menu Tortilla (100 % whole grain)	2 (85 g)	744 (Environmental Defence Canada, 2018)	63.2
Salsa	2 tbsp	_	_
Ground beef (grain fed and finished)	1/2 cup (75 g)	5000 ^a (40 CFR 180.364(a)(2) (USEPA), 1980)	375
Mozzarella cheese Carrot/celery sticks	2 oz 1 cup	-	_
Snack			
Tim Hortons glazed Timbit	6 (150 g–25 g each)	209 (Environmental Defence Canada, 2018)	31.4
Decaf coffee Honey	1 cup 1 tbsp (21	- 64 (Vainshelboim, 2015)	- 1.34
365 coffee cream	g) 2 tbsp (30	104 (TriplePundit, 2016)	3.12
ooo conce cream	g)	To I (Triplet alidit, 2010)	0.12
Dinner			
Grilled salmon	4 oz	-	-
Lentil salad Green beans	1/2 cup (80 g)	284 (Institute for Responsible Technology, 2022)	22.7
Teriyaki sauce (with soy)	1 cup 2 tsp. (8 g)	242 (Pesticide Action Network International, n.d.)	1.93
Apple crisp made with oatmeal	1/2 cup (50 g)	135 (Environmental Defence Canada, 2018)	6.75
Water	No limit	-	-
Snack			
Ritz crackers	10 (32 g)	5695 (A Survey on the Uses of Glyphosate in European Countries, n.d.)	18.2
Cream cheese	2 tbsp	_	_
Apple, sliced	1/2 medium	-	-
Total (µg/day) Total (mg/kg/day)			603.02 0.01

^a Maximum Allowable Amount.

Table 2Glyphosate levels in commercially available foods and laboratory rodent chow using our modified UPLC detection method.

Sample Matrix	Concentration of Glyphosate $(\mu g/g)$	Concentration Glyphosate (ppb)
Red Lentils Picolab® 5053 Mouse Diet	0.245 0.381	245 381
Desiccated Wheat Nondesiccated Wheat	2.445 ND	2445 ND

4.3. Animal husbandry

Mice were housed under specific pathogen-free conditions within the bioscience facility at UBC Okanagan. The UBC Animal Care Committee approved all animal experiments under protocols A22-0231 and A18-0317. Mice were kept on ventilated racks and housed at 22 \pm 2 $^{\circ}$ C with controlled humidity on a 14 h:10 h light: dark cycle and provided with autoclaved woodchips, crinkle paper, and polycarbonate houses for cage enrichment. Parental generation $Muc2^{+/-}$ and $Muc2^{-/-}$ mice were bred in-house. Original $Muc2^{-/-}$ mice used to generate our colony were obtained from Dr. Bruce Vallance at UBC Vancouver and were derived on a C57Bl/6 background. To mitigate cage effects, we bred heterozygous ($Muc2^{+/-}$) with homozygous ($Muc2^{-/-}$) mice, thereby creating cohoused littermates who were healthy ($Muc2^{+/-}$) and colitis-susceptible $(Muc2^{-/-})$. This has been shown to be an optimal method for microbiome standardization. Within our facility, we have shown that $Muc2^{+/-}$ are healthy and do not develop colitis or any metabolic or behavioral abnormalities associated with a total knockout of Muc2 and therefore. served as our healthy population. A comparison of $Muc2^{+/+}$, $Muc2^{+/-}$ and $Muc2^{-/-}$ mice in our facility can be found in (Fig. S1, A–D). To reduce stress-induced litter loss, F0 dams were not phenotyped during gestation or lactation. All F0 animals were monitored for general health and maintained under identical housing and diet conditions beginning two weeks prior to mating.

4.4. Sample size justification

Given the unique animal model, breeding scheme, and proprietary dose used in this study, it was impossible to collect the effect size and standard deviation from literature. Therefore, we estimated sample size using the resource equation approach (Arifin and Zahiruddin, 2017; Festing and Altman, 2002; Charan and Kantharia, 2013; Mead et al., 2012; Festing, 2006). In brief, the resource equation is based on the law of diminishing returns. It assumes that the acceptable range of degrees of freedom (DF) for the error term within an analysis of variance (ANOVA) is between 10 and 20. For one-way ANOVA, the within-subject DF can be determined as:

$$n = \frac{DF}{k} + 1$$

where:

k is the number of groups

n is the number of subjects per group.

Based on the acceptable range of the DF, the DF in the formula is replaced with the minimum (10) and maximum (20) to obtain the minimum and maximum numbers of animals per group. Therefore, the minimum and maximum number of animals needed for the current study was estimated for k = 5 groups (Baseline Exposure, Average American Diet F1, Average American Diet F2, EPA Upper Limit F1 and EPA Upper Limit F2). Using the equation above, it was determined that each group requires a minimum of three animals and a "maximum" of five per genotype. However, it should be noted that the resource equation is not as robust as the power analysis method, and every effort was made to include more than the maximum number of animals required per group. To evaluate statistical power, we conducted a post-hoc ANOVA-based power analyses using representative metrics across key phenotypic domains: open field distance (behavior), oral glucose tolerance (metabolic), mucin2 gene expression, and histological scores. Power calculations (G*Power 3.1) based on observed effect sizes (Cohen's f: 0.73–1.31) and total sample sizes (N = 45-59, 5 groups) indicate power \geq 97 % for each analysis (see Table S7), supporting the adequacy of the sample sizes to detect transgenerational differences.

4.5. Experimental design

weaned, breeding mice were sacrificed, and tissues were collected as outlined previously. Each mouse was considered to be an experimental

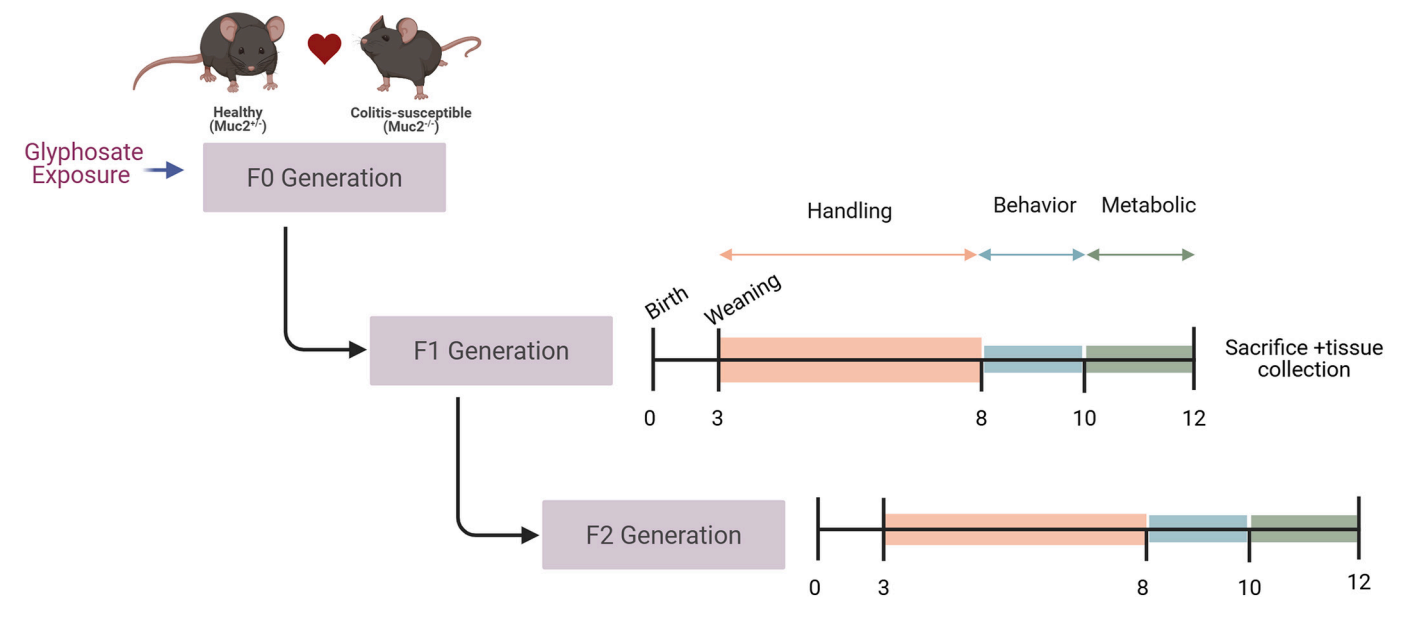


Fig. 6. Experimental design.

Upon reaching sexual maturity (6 weeks of age), breeding pairs consisting of $Muc2^{+/-}$ (healthy) and $Muc2^{-/-}$ (colitis-susceptible) mice were established. A summary of parental generation sex and genotype combinations can be found in Table S2. Non-exposed mice received autoclaved reverse-osmosis water ad libitum. F0 breeders began receiving glyphosate-supplemented water at sexual maturity and exposure continued through mating, and gestation. Glyphosate-exposed mice received autoclaved reverse-osmosis water with glyphosate N-(phosphonomethyl)glycine (96 %, Millipore Sigma, Cat ID: 337757) at either the AAD dose (0.01 mg/kg body weight/day) or the current ADI set by the EPA (1.75 mg/kg body weight/day), ad libitum. Unexposed animals were generated in parallel with exposed cohorts and tested within the same experimental windows to minimize batch effects across generations. Researchers were not blinded with regards to treatment, however, experimenters were blind with regards to genotype of animals within the cage as genotyping occurred at the end of the experiment. All mice received irradiated PicoLab® Mouse Diet 5058 ad libitum. At six weeks of age, offspring were assigned using a random number generator to one of two groups: experimental or breeding. Care was taken to ensure that random assignment occurred with no sibling or cousin breeding to avoid inbreeding. Breeding mice were used to generate the F2 generation, whereas experimental mice were handled weekly until seven weeks of age and then daily for one week before behavior testing began. Mice in the experimental group began behavior testing at eight weeks and metabolic testing at ten weeks. Mice were sacrificed at 12 weeks of age. In brief, mice were anesthetized to the surgical plane using isoflurane, and cardiac blood was collected via cardiac puncture. The time between cage disturbance and death was <3 min, as exceeding that time elicits stress hormone production (Hamden et al., 2021). Death was confirmed using cervical dislocation, and the distal colon, ileum, stool, cecum, and liver were collected for analysis. Both the distal colon and ileum were divided into three pieces, with one piece being flash-frozen in liquid nitrogen and stored at $-80\ ^{\circ}\text{C}$ for microbiome analysis, one stored in RNAprotect (Qiagen, Cat ID: 76106) for mRNA analysis, and the third in 10 % neutral buffered formalin (Fisher Scientific, Cat ID: 23-305510) for histopathological analysis. The collected cardiac blood was spun for 15 min at 1500g to isolate the serum. Once F2 generation pups were unit. No metabolic or behavioral phenotyping was conducted on F0 breeders to avoid introducing stress-related variability or confounds during mating, gestation, and lactation. All outcomes were assessed exclusively in F1 and F2 offspring to isolate effects of prenatal exposure and potential intergenerational transmission.

4.6. Open field test

At eight weeks of age, mice were habituated to the testing room for 1 h before test initiation. The open field setup comprised a single 40 cm \times 40 cm \times 40 cm arena made of opaque white, non-reflective acrylic material (Conduct Science). The box was cleaned with 10 % ethanol before and between sessions, reducing stress odors and olfactory cues. A video camera (GoPro Hero 8) recorded the mouse activity within the open field. Mice were placed in the center of the open field, and their activity was recorded for 10 min. The testers positioned themselves outside the mice's field of view, and mice were monitored remotely using the GoPro Quik App (version 12.4.1, Apple iPhone iOS). Video footage was analyzed using EthoVision XT (version 17; Noldus) for the number of center square entries, time spent within the center square, distance travelled, body velocity, rearing frequency, and time spent grooming. Data were collected from two independent experiments.

4.7. Radial arm maze

Mice were assessed using the fully baited training procedure where each arm chamber contained a food reward, and the mouse was expected to learn to visit each arm only once per session. Once the mouse had obtained the food reward from an arm, re-entry into the now unabaited arm is considered a memory error. The radial arm maze test was performed over four consecutive days. Visual cues outside the maze remained constant over the four days to allow the mice to establish a mental map of the maze. Because mice are neophobic, treats were provided to mice in their home cages three days before testing began. Day 1: The mice were habituated to the maze and allowed to explore it freely for 10 min. Days 2–4: Mice were placed in the center of the radial arm maze until task completion was achieved. Task completion was defined

as entry into each arm of the maze or 10 min had elapsed. Mice were monitored remotely to determine the number of times an arm had been entered (memory errors). The total number of memory errors was averaged over three consecutive trials.

4.8. Light/dark test

Forty-eight hours after open-field testing, the mice were again habituated to the testing room for 1 h before test initiation. The light/dark setup consisted of a single 40 cm \times 40 cm box divided into two compartments, with one being open to the light and the other being dark (light compartment: 25 cm \times 40 cm, dark compartment: 17.5 cm \times 40 cm) (Conduct Science). Mice were placed in the center of the light section of the light/dark maze, and their activity was recorded for 10 min (GoPro Hero 8). The observers positioned themselves outside the mouse's view, and the maze was wiped with 10 % ethanol before each session and between sessions, as described above. An impartial, blinded individual manually analyzed the video footage. Metrics measured included the time spent in the dark, the number of transitions between light and dark, and the latency to enter the dark compartment.

4.9. Oral glucose tolerance test

Mice were fasted for 6 h before the start of the test, which has been shown to be optimal in rodents (Andrikopoulos et al., 2008). Fasting blood glucose readings were obtained from blood samples collected from a tail poke and quantified using a OneTouch Verio Flex® glucometer. Before testing, the glucometer was calibrated using the control solution provided by the manufacturer. A 30 % glucose solution was prepared using D-(+)-Glucose (Sigma-Aldrich, Cat ID: 50-99-7) prepared in phosphate-buffered saline and sterile-filtered using a 0.2-micron syringe filter. Following the fasting blood glucose reading, mice received glucose gavage at a dose equal to 2 g/kg fasted body weight. Blood glucose readings were collected 15, 30, 60, and 120 min after gavage. The area under the curve (AUC) was determined using the trapezoid rule.

4.10. Insulin tolerance test

Mice were fasted for 6 h before the start of the test. Initial blood glucose readings were obtained as described above. Human insulin (Humalog®, 100 U/mL) was diluted to a 0.1 U/mL working solution by sterile isotonic saline. Following the initial blood glucose reading, the mice received an intraperitoneal insulin injection dose equal to 0.5 U/kg fasted body weight. Blood glucose readings were collected 15-, 30-, 60-, and 120 min after injection. If at any time a mouse became hypoglycemic, defined as a blood glucose reading less than 2.3 mmol/L, or if blood glucose levels failed to return to normal following 120 min, mice received a bolus intraperitoneal injection of a 30 % sucrose solution (Sigma-Aldrich, Cat ID: 57-50-1) and were removed from the remainder of the test. AUC was determined using the trapezoid rule.

4.11. Histopathological scoring

Tissues collected for histology were immediately placed in 10 % neutral buffered formalin. Following 24-h formalin fixation, the tissues were washed in phosphate-buffered saline (PBS) and stored at 4 $^{\circ}$ C in 70 % ethanol. Tissues were sent to BC Children's Hospital Research Institute for paraffin embedding, sectioning, and hematoxylin and eosin (H&E) staining. Coded samples, blinded to the scorers, were evaluated and scored by three people, and scores were averaged. Samples were collected from two independent experiments. Scoring parameters used can be found in Tables S3 and S4.

4.12. Immunohistochemistry

Tissues were collected as outlined above. Unstained paraffin slides were cut for immunohistochemistry. Slides were deparaffinized in xylene (two five-minute washes), and tissues were rehydrated using a series of ethanol washes ranging from 100 % to 70 % ethanol before being rinsed in deionized water and PBS. Tissues were then incubated with trypsin (Sigma-Aldrich Cat-ID: 9002-07-7) at 37 °C for 30 min to facilitate antigen retrieval. Following antigen retrieval, a blocking solution of 5 % IgG-free bovine serum albumin (BSA) (Sigma-Aldrich Cat-ID: 9048-46-8) was applied, and slides were incubated for 20 min at room temperature. A primary antibody solution (F4/80: Cedarlane, Cat-ID: CL89170AP, MPO: Invitrogen, Cat-ID: PA516672, ZO2: Invitrogen, Cat-ID: 71-1400) was applied at a 1:50 antibody: BSA dilution ratio and slides were incubated overnight at 4 $^{\circ}\text{C}$. After incubation, slides were rinsed in PBS. A fluorescently conjugated secondary antibody (F4/80: Invitrogen, Cat-ID: A11006, MPO: Invitrogen, Cat-ID: A11012, ZO2: Invitrogen, Cat-ID: A-11008) was applied at a 1:1000 antibody: BSA dilution ratio and incubated at room temperature for 1 h. Following incubation, a histology mounting medium containing 4'-6-diamidino-2phenylindole (DAPI) was applied (Sigma-Aldrich Cat-ID: F6182) and a coverslip was applied. Slides were imaged using the EVOS M500 cell imaging system (ThermoFisher Cat-ID: AMF5000SV). Cells were quantified using QuPath (version 0.4.4) using positive cell detection to ensure cells counted colocalized both fluorescent signals (DAPI stained nucleus and fluorescently stained structure of interest).

4.13. RNA sample preparation

Total RNA was extracted from colon tissue using the RNeasy Fibrous Tissue Mini Kit (Qiagen, Cat ID: 74704) according to the manufacturer's instructions. 2-mercaptoethanol (Sigma-Aldrich, Cat ID: M6250) was added to the lysis buffer to protect against RNase degradation. To minimize potential batch effects, all kits were ordered simultaneously, and samples were randomized across kits. Immediately following extraction, purified RNA was quantified spectrophotometrically (ThermoFisher, Nanodrop 2000), normalized to 250 ng/ μ L and cDNA was synthesized using an iScript Reverse Transcription kit (BioRad, Cat ID: 1708890) according to the manufacturer's instructions with 500 ng RNA per reaction. cDNA was diluted to a final concentration of 5 ng/ μ L for downstream analysis. All samples were collected from two independent experiments.

4.14. Quantitative real-time PCR

Relative gene expression was quantified using quantitative real-time PCR (qPCR). The 10 μL reaction consisted of 0.4 μL of each forward and reverse primer (10 mM), 5 μL SsoAdvanced Universal SYBR Green Supermix (Bio-Rad, Cat ID: 1725210), 3.2 μL DNase-free water and 1 μL cDNA template. Samples were assigned to a plate using a random number generator to mitigate batch effects. Samples were run in duplicate using primers separated by at least one intron on the corresponding genomic DNA to prevent amplification of genomic DNA when possible; for primers not separated by one intron, controls containing no reverse transcriptase were run to ensure that there was no amplification of genomic DNA. A list of primer sequences can be found in Table S5.

4.15. Relative gene expression

Relative gene expression was determined using Bio-Rad CFX Manager software (version 2.1, Hercules, California, USA). The relative normalized expression was determined by dividing the relative expression of the gene of interest by the geometric mean of the relative expression of the reference genes. The log of the relative normalized expression is equivalent to the $\Delta\Delta$ Cq. The reference genes *Eef2* and *Tbp* were used as they are stable within the gut during inflammation (Eissa

et al., 2016). Primer efficiencies for each assay were determined using LinRegPCR (version 2021.2), which uses the slope of the exponential phase of each reaction to determine the least variable mean PCR efficiency per assay. This is superior to the standard curve method as it allows for a more precise determination of amplification efficiency and is more sensitive in detecting slight differences in the initial amount of template. Additionally, LinReg can provide reliable quantification in the presence of minor experimental variations (e.g., reaction efficiency, primer-dimer formation). qPCR data were generated using a Bio-Rad C1000 Touch Thermal Cycler (CFX96) and analyzed using Bio-Rad CFX Manager Software version 2.1 (Hercules, California, USA). Quality control measures were conducted on each run, including excluding or rerunning samples with any of the following criteria: negative control Cq values less than 38, primer efficiency below 90 % or above 110 %, or replicate group standard deviation greater than 0.20.

4.16. Cytokine network analysis

Cytokine network analysis was conducted in R Studio (version 2023.09.01 Build 494) running R (version 4.3.1) using packages *tidyverse* and *factoextra*.

4.17. Serum hormone and metabolite analysis

Blood was collected from mice via cardiac puncture. The serum was isolated by allowing the blood to clot at room temperature for 20 min before spinning at 1500 g for 15 min. A protease inhibitor cocktail (Amresco, Cat ID: M221) was added to the sera before being stored at $-80\,^{\circ}\mathrm{C}$ for analysis. Serum samples that were hemolyzed or lipemic were not used. Serum samples were diluted 2-fold with sterile PBS (pH = 7.5). Serum was sent to Eve Technologies (Calgary, AB, Canada) and analyzed for metabolic hormones (Mouse Metabolic Array) using addressable laser bead immunoassay.

Tryptophan pathway metabolites, including tryptophan, kynurenine, serotonin and the microbial indole derivatives indole-aldehyde and 3-indolepropionic acid, were quantified by GC-MS following derivatization (methoxylamine hydrochloride and MSTFA) at Innovate Phytoceuticals (Kelowna, BC).

4.18. Enzyme-linked immunosorbent assay (ELISA) analysis

Serum corticosterone levels were quantified using the 96-well Corticosterone Multi-Format ELISA kit (Arbor Assays, Cat ID: K014-H5). Serum samples were collected, aliquoted, and stored at $-80\,^{\circ}\mathrm{C}$ before analysis. Serum samples that were hemolyzed or lipemic were not used. All samples were diluted 100-fold before use. This kit is sensitive to 20.9 pg/mL using 50 L input. All samples were randomly assigned to a plate using random number generation and were run in duplicate according to the manufacturer's specifications. Plates were read at 450 nm, and baseline optical density correction was conducted at 620 nm. Concentrations were determined using MyAssays (MyAssays.com).

4.19. Microbiome sample preparation

Total microbial DNA was isolated from colon tissues using the QIAmp PowerFecal Pro DNA Kit (Qiagen, Cat ID: 51804). All kits were ordered simultaneously, and samples were randomized across kits to minimize potential batch effects. In brief, samples were added to the PowerBead Pro Tube™ and homogenized for 20 min using a vortex adapter (Qiagen, Cat ID:13000-V1-24). The rest of the extraction was conducted according to the manufacturer's specifications, except for an additional wash with the included ethanol-based wash solution to improve sample purity. DNA was quantified spectrophotometrically (ThermoFisher, Nanodrop 2000). A mock community provided by Integrated Microbiome Platforms for Advancing Causation Testing and Translation (IMPACTT) (Calgary, AB, Canada) was also extracted along

with samples and sent for sequencing. Samples were collected from two independent experiments.

4.20. 16S rRNA sequencing

DNA samples were sent to Gut4Health (BC Children's Hospital Research Institute, Vancouver, BC) for library prep and 16s sequencing. In brief, the V4 region of the 16s gene was amplified with barcode primers containing the index sequences using a KAPA HiFi HotStart Real-time PCR Master Mix (Roche). PCR product amplification and concentration were monitored using a Bio-Rad CFX Connect Real-Time PCR system. Amplicon libraries were then purified, normalized, and pooled using the SequalPrepTM normalization plate (Applied Biosystems). According to the manufacturer's instructions, library concentrations were verified using a Qubit™ dsDNA high-sensitivity assay (Invitrogen) and KAPA Library Quantification Kit (Roche). The purified pooled libraries were submitted to the Bioinformatics and Sequencing consortium at UBC Vancouver, which verified DNA quality and quantity using an Agilent high-sensitivity DNA kit on an Agilent 2100 Bioanalyzer. Sequencing was performed on the Illumina MiSeqTMv2 platform with 2×250 paired-end read chemistry.

4.21. Bioinformatics

All bioinformatic processes were performed using a combination of R statistical software and QIIME 2 (version 2023.9) using the various built-in plugins described below. Demultiplexed sequences obtained from the sequencing facility underwent quality control and denoising using DADA2. Forward and reverse reads were truncated at 240 bases. Taxonomy was assigned to sequences using a pre-trained Naïve Bayes classifier trained on the Greengenes version 2 classifier (version 2022.10.backbone.v4). Differential abundance testing and effect size of taxa abundances were conducted using LEfSe, where features with fewer than ten counts across all samples or appearing in fewer than five samples were removed. A multiclass comparison was performed using a Kruskal-Wallis test ($\alpha = 0.05$), and a linear discriminant analysis (LDA) score for discriminative features was set to 2.0. Biologically relevant features were visualized in a cladogram. BugBase was used to predict high-level community phenotypes present within samples. For BugBase analysis, VSEARCH was used to filter the feature table generated by DADA2 using a closed-reference approach. Samples were filtered using the Greengenes reference database (version 13.8) and 97 % clustering. Using denoised 16S amplicon variants (from OIIME2/DADA2), the Phylogenetic Investigation of Communities by Reconstruction of Unobserved States (PICRUSt2-v2.6.0) program was utilized to predict metabolic functions and pathway abundances based on the Kyoto Encyclopedia of Genes and Genomes (KEGG) and MetaCyc database, employing the default pipeline. Predicted pathway abundances were normalized to gene copy number. To assess differences across exposure groups (Baseline exposure, AAD, EPA) and generations (F1 vs. F2), ALDEx2 (v1.28.1) in R was applied to the pathway table. p-values were adjusted using the Benjamini–Hochberg method, and FDR < 0.05 was considered significant.

4.22. Statistical analysis

All statistical analysis was conducted in GraphPad Prism (version 10) unless otherwise specified. Data displaying a log-normal distribution were log-transformed before outlier detection and statistical analysis and is displayed in its log-transformed version. Outliers were detected using the ROUT method with $Q=1\,\%$. Statistical assumptions, including normality and homogeneity of variance, were tested using D'Agostino-Pearson omnibus (K2) and Bartlett's test, respectively, and these tests were used to determine which statistical test was used. Multiple comparisons were corrected by controlling the false discovery rate using the two-stage step-up method of Benjamini, Krieger and Yekutieli. For

parametric tests, effect size was calculated using the method described by Keppel and Wickens and is reported as partial eta squared $(\eta^2 p)$ (Keppel and Wickens, 2004). For non-parametric tests, eta-squared (η^2) was calculated manually using the formula:

$$\eta 2 = \frac{H - k + 1}{N - k}$$

where:

H is the Kruskal-Wallis test statistic.

k is the number of groups.

N is the total number of observations across all groups.

A result was considered significant with an adjusted *p*-value \leq 0.05. Results with an adjusted p-value ≤ 0.08 were considered a nonsignificant trend. Confidence intervals (CI) reported represent the 95 % confidence interval. Due to the inherent unpredictability of mouse breeding, we were unable to obtain sufficient numbers of each sex within each generation and genotype to achieve the statistical power needed for a detailed analysis of sex differences. To address this limitation, we conducted an exploratory analysis of potential sex effects using a permutational multivariate analysis of variance (PERMANOVA) with 999 permutations, implemented via the adonis2 function in the vegan R package. This analysis assessed the influence of group, sex, and group × sex interactions, using Euclidean distance metrics. The reported PERMANOVA *p*-values represent the combined effects of group and sex. The feature table was transformed to centered log-ratio (CLR) to normalize compositional data. The correlation between each hormone and the CLR-transformed abundances of differentiated bacteria was assessed using Spearman's rank correlation, followed by an exposureadjusted partial correlation analysis, which involved regressing each variable on groups and examining the rank residuals. To evaluate the influence of glyphosate exposure across groups (Baseline Exposure, AAD F1, AAD F2, EPA F1, EPA F2), we performed an analysis of covariance (ANCOVA) with interaction term for bacteria CLR-abundance \times groups in addition to main effects to evaluate slope heterogeneity. Two-way ANCOVA models included main effects of dose (no exposure, AAD, EPA) and generation (baseline, F1, F2), along with their interaction term (dose \times generation), to assess how the effect of glyphosate dose varies across generations. For dose-response relationships, dose was encoded as an ordered numeric variable reflecting the administered glyphosate in water (0, 0.01 mg, 1.75 mg), and trends were examined using Jonckheere-Terpstra (JT) tests within F1 and F2, reporting JT p-values with a permutation-based implementation to account for ties and small group sizes for monotonic increases or decreases across Control to AAD to EPA. All analyses were conducted in R (version 4.4.2) using the following packages:phyloseq, clinfun, tidyverse, pheatmap, emmeans, and ggplot2.

CRediT authorship contribution statement

J.A. Barnett: Writing – original draft, Methodology, Investigation, Formal analysis, Data curation, Conceptualization. J.K. Josephson: Writing - review & editing, Data curation. E. Yuzbashian: Writing review & editing, Data curation. N. Haskey: Writing - review & editing, Methodology. M.M. Hart: Writing - review & editing, Conceptualization. K.K. Soma: Writing – review & editing, Methodology. A. Verdugo: Writing - review & editing, Data curation. C.J. McComb: Writing review & editing, Data curation. M.L. Bandy: Writing - review & editing, Formal analysis. S. Ghosh: Writing - review & editing, Methodology. C. Letef: Writing – review & editing, Data curation. A. Copp: Writing – review & editing, Data curation. R. Ishida: Writing – review & editing, Data curation. J. Gibon: Writing - review & editing, Methodology. J. Ye: Writing - review & editing, Data curation. R.T. Giebelhaus: Writing - review & editing, Methodology, Data curation. S.J. Murch: Writing - review & editing, Methodology, Data curation. M.M. Jung: Writing - review & editing, Methodology, Data curation. D.L.

Gibson: Writing – review & editing, Supervision, Methodology, Funding acquisition, Conceptualization.

Declaration of competing interest

Authors declare that they have no competing interests.

Acknowledgements

We would like to thank our funders, including crowdfunding UBC, the Natural Sciences and Engineering Research Council (NSERC) who supported this work through both a discovery grant to D.L.G., and an Alliance collaborative grant to D.L.G, M.M.H and S.M and graduate student funding awarded to J.A.B. Thank you to those who contributed to our crowdfunding campaign, who helped us fund preliminary pilot rodent studies. Thank you to April Mahovlic for her assistance characterizing the $Muc2^{+/-}$ and $Muc2^{-/-}$ models. Thank you to Christian Mustapich for his assistance with light/dark video analysis. Thank you to Ryan Bonnie and Helen Chiang for their assistance during mouse experiments. Thank you to AC for their intellectual contribution early in the project. Thank you to Dr. Wesley Zandberg for the use of his lyophilizer for cecal samples used in SCFA analysis. Fig. 5 was created in https://BioRender.com.

Appendix A. Supplementary data

Supplementary data to this article can be found online at https://doi.org/10.1016/j.scitotenv.2025.180437.

Data availability

The 16S sequences files and metadata used for the analysis of this study are publicly available at: https://osf.io/7wyc4/?view_only=268c92d8f5f24d8db1afab154a3e4723 (DOI 10.17605/OSF.IO/7WYC4).

References

- 40 CFR 180.364(a)(2) (USEPA), 1980. U.S. National Archives and Records Administration's Electronic Code of Federal Regulations. Available from, as of September 8, 2014. https://www.ecfr.gov.
- A Survey on the Uses of Glyphosate in European Countries. Le Centre pour la Communication Scientifique Directe. May 2020. doi:10.15454/a30k-d531.
- Andrikopoulos, S., Blair, A.R., Deluca, N., Fam, B.C., Proietto, J., 2008. Evaluating the glucose tolerance test in mice. Am. J. Physiol. Endocrinol. Metab. 295 (6), E1323–E1332. https://doi.org/10.1152/ajpendo.90617.2008.
- Arifin, W.N., Zahiruddin, W.M., 2017. Sample size calculation in animal studies using resource equation approach. The Malaysian Journal of Medical Sciences: MJMS 24 (5), 101–105. https://doi.org/10.21315/mjms2017.24.5.11.
- Barnett, J.A., Gibson, D.L., 2020. Separating the empirical wheat from the pseudoscientific chaff: A critical review of the literature surrounding glyphosate, dysbiosis and wheat-sensitivity. Front. Microbiol. 11, 556729–556729. https://doi. org/10.3389/fmicb.2020.556729.
- Barnett, J.A., Bandy, M.L., Gibson, D.L., 2022. Is the use of Glyphosate in modern agriculture resulting in increased neuropsychiatric conditions through modulation of the gut-brain-microbiome axis? Front. Nutr. 9, 827384. https://doi.org/10.3389/ fnut.2022.827384.
- Beckie, H.J., Flower, K.C., Ashworth, M.B., 2020. Farming without glyphosate? Plants (Basel) 9 (1), 96. https://doi.org/10.3390/plants9010096.
- Bloem, B.R., Boonstra, T.A., 2023. The inadequacy of current pesticide regulations for protecting brain health: The case of glyphosate and Parkinson's disease. The Lancet Planetary Health 7 (12), e948–e949. https://doi.org/10.1016/S2542-5196(23) 00255-3
- Buchenauer, L., Junge, K.M., Haange, S.B., Simon, J.C., von Bergen, M., Hoh, A.L., Aust, G., Zenclussen, A.C., Stangl, G.I., Polte, T., 2022. Glyphosate differentially affects the allergic immune response across generations in mice. Sci. Total Environ. 850, 157973. https://doi.org/10.1016/j.scitotenv.2022.157973.
- Canadian Food Inspection Agency, 2017. Safe gaurding With Science: Glyphosate Testing in 2015-2016. https://inspection.canada.ca/DAM/DAM-food-aliments/STAGING/text-texte/chem_testing_report_2015-2016_glyphosate_srvy_rprt_1491855525292_eng.pdf.
- Cani, P.D., Knauf, C., 2021. A newly identified protein from akkermansia muciniphila stimulates GLP-1 secretion. Cell Metab. 33 (6), 1073–1075. https://doi.org/ 10.1016/j.cmet.2021.05.004.

- Carrera-Bastos, P., Fontes-Villalba, M., O'Keefe, J.H., Lindeberg, S., Cordain, L., 2011. The western diet and lifestyle and diseases of civilization. Res. Rep. Clin. Cardiol. 2 (default), 15–35. https://doi.org/10.2147/RRCC.S16919.
- Cecco, L., 2023. Canadian government urged to test sick patients for herbicide. March 1, The Guardian. https://www.theguardian.com/environment/2023/mar/01/canadia n-government-urged-to-test-sick-patients-for-herbicide.
- Charan, J., Kantharia, N.D., 2013. How to calculate sample size in animal studies? J. Pharmacol. Pharmacother. 4 (4), 303–306. https://doi.org/10.4103/0976-500X.119726.
- Chow, J., Tang, H., Mazmanian, S.K., 2011 Aug. Pathobionts of the gastrointestinal microbiota and inflammatory disease. Curr. Opin. Immunol. 23 (4), 473–480. https://doi.org/10.1016/j.coi.2011.07.010. Epub 2011 Aug 17. PMID: 21856139; PMCID: PMC3426444.
- Clemente-Suárez, V.J., Beltrán-Velasco, A.I., Redondo-Flórez, L., Martín-Rodríguez, A., Tornero-Aguilera, J.F., 2023. Global impacts of western diet and its effects on metabolism and health: a narrative review. Nutrients 15 (12), 2749. https://doi.org/ 10.3300/mu15122749
- Dadlani, A., Gala, K., Rai, J., Rai, S., Dryden, G., 2021. P027 brain fog in patients with inflammatory bowel disease, and association with use of probiotics. Am. J. Gastroenterol. 116 (Suppl. 1), S7. https://doi.org/10.14309/01. pi.g.007097097082085-0
- Drzyzga, D., Lipok, J., 2018. Glyphosate dose modulates the uptake of inorganic phosphate by freshwater cyanobacteria. J. Appl. Phycol. 30 (1), 299–309. https:// doi.org/10.1007/s10811-017-1231-2.
- Eissa, N., Hussein, H., Wang, H., Rabbi, M.F., Bernstein, C.N., Ghia, J.E., 2016. Stability of reference genes for messenger RNA quantification by Real-Time PCR in mouse dextran sodium sulfate experimental colitis. PloS One 11 (5), e0156289. https://doi.org/10.1371/journal.pone.0156289.
- Environmental Defence Canada, 2018, September. What's in your lunch? Glyphosate report. https://environmentaldefence.ca/wp-content/uploads/2018/09/Whats-In-Your-Lunch-Glyphosate-Report-Sept-2018.pdf.
- Eriguchi, M., Iida, K., Ikeda, S., Osoegawa, M., Nishioka, K., Hattori, N., Nagayama, H., Hara, H., 2019. Parkinsonism relating to intoxication with glyphosate. Intern. Med. 58 (13), 1935–1938. https://doi.org/10.2169/internalmedicine.2028-18.
- Eskenazi, B., Gunier, R.B., Rauch, S., Kogut, K., Perito, E.R., Mendez, X., Limbach, C., Holland, N., Bradman, A., Harley, K.G., Mills, P.J., Mora, A.M., 2023. Association of lifetime exposure to glyphosate and aminomethylphosphonic acid (AMPA) with liver inflammation and metabolic syndrome at young adulthood: findings from the CHAMACOS study. Environ. Health Perspect. 131 (3), 37001. https://doi.org/ 10.1289/EHP11721.
- Feng, X., Wang, M., Wang, Y., et al., 2025. Associations between environmental glyphosate exposure and glucose homeostasis indices in US general adults: a national population-based cross-sectional study. Sci. Rep. 15, 1627. https://doi.org/10.1038/ s41598-024-84694-5
- Festing, M.F.W., 2006. Design and statistical methods in studies using animal models of development. ILAR J. 47 (1), 5–14. https://doi.org/10.1093/ilar.47.1.5.
- Festing, M.F.W., Altman, D.G., 2002. Guidelines for the design and statistical analysis of experiments using laboratory animals. ILAR J. 43 (4), 244–258. https://doi.org/10.1093/ilar.43.4.244.
- Hamden, J.E., Salehzadeh, M., Gray, K.M., Forys, B.J., Soma, K.K., 2021. Isoflurane stress induces glucocorticoid production in mouse lymphoid organs. J. Endocrinol. 251 (2), 137–148. https://doi.org/10.1530/JOE-21-0154.
- Hill, C.E., Myers, J.P., Vandenberg, L.N., 2018. Nonmonotonic dose–response curves occur in dose ranges that are relevant to regulatory decision-making. Dose-Response 16 (3), 1559325818798282. https://doi.org/10.1177/1559325818798282.
- Hopkins, C.W.P., Powell, N., Norton, C., Dumbrill, J.L., Hayee, B., Moulton, C.D., 2021. Cognitive impairment in adult inflammatory bowel disease: A systematic review and meta-analysis. Journal of the Academy of Consultation-Liaison Psychiatry 62 (4), 387–403. https://doi.org/10.1016/j.psym.2020.10.002.
- 387–403. https://doi.org/10.1016/j.psym.2020.10.002.
 Institute for Responsible Technology, 2022. Glyphosate database. August 26. https://responsibletechnology.org/wp-content/uploads/2022/10/Glyphosate-Database-PDF_2022-0826.pdf.
- Ishioh, M., Nozu, T., Igarashi, S., Tanabe, H., Kumei, S., Ohhira, M., Okumura, T., 2020. Ghrelin acts in the brain to block colonic hyperpermeability in response to lipopolysaccharide through the vagus nerve. Neuropharmacology 173, 108116. https://doi.org/10.1016/j.neuropharm.2020.108116.
- Kang, Y., Park, H., Choe, B., Kang, B., 2022. The role and function of mucins and its relationship to inflammatory bowel disease. Front. Med. 9, 848344. https://doi.org/ 10.3389/fmed.2022.848344.
- Keppel, G., Wickens, T.D., 2004. Design and Analysis: A Researcher's Handbook. Pearson Prentice Hall.
- Koch, D.G., 2023. High levels of glyphosate in most patients with 'atypical neurological diseases': Open letter. July 13, NB Media Co-op. https://nbmediacoop.org/2023/07/13/high-levels-of-glyphosate-other-pesticides-in-most-patients-with-atypical-neurological-disease-letter/.
- Kopp, W., 2019. How western diet and lifestyle drive the pandemic of obesity and civilization diseases. Diabetes Metab. Syndr. Obes. 12, 2221–2236. https://doi.org/ 10.2147/DMSO.S216791.
- Liñán-Rico, Andromeda, Turco, Fabio, Ochoa-Cortes, Fernando, Harzman, Alan, Needleman, Bradley J., Arsenescu, Razvan, Abdel-Rasoul, Mahmoud, Fadda, Paolo, Grants, Iveta, Whitaker, Emmett, Cuomo, Rosario, Christofi, Fievos L., 2016. Molecular Signaling and Dysfunction of the Human Reactive Enteric Glial Cell Phenotype: Implications for GI Infection, IBD, POI, Neurological, Motility, and GI Disorders. Inflammatory Bowel Diseases 22 (8), 1812–1834. https://doi.org/ 10.1097/MIB.00000000000000854, 1 August.

- Mead, R., Gilmour, S.G., Mead, A., 2012. Statistical Principles for the Design of Experiments: Applications to Real Experiments, 1st ed. Cambridge University Press. https://doi.org/10.1017/CBO9781139020879.
- Mirpuri, J., 2021 Jan. Evidence for maternal diet-mediated effects on the offspring microbiome and immunity: implications for public health initiatives. Pediatr. Res. 89 (2), 301–306. https://doi.org/10.1038/s41390-020-01121-x. Epub 2020 Sep 12. PMID: 32919391; PMCID: PMC7897208.
- Morampudi, V., Dalwadi, U., Bhinder, G., Sham, H.P., Gill, S.K., Chan, J., Bergstrom, K.S. B., Huang, T., Ma, C., Jacobson, K., Gibson, D.L., Vallance, B.A., 2016. The goblet cell-derived mediator RELM- β drives spontaneous colitis in Muc2-deficient mice by promoting commensal microbial dysbiosis. Mucosal Immunol. 9 (5), 1218–1233. https://doi.org/10.1038/mi.2015.140.
- Mulligan, C.M., Friedman, J.E., 2017 Oct. Maternal modifiers of the infant gut microbiota: metabolic consequences. J Endocrinol. 235 (1), R1–R12. https://doi. org/10.1530/JOE-17-0303. Epub 2017 Jul 27. PMID: 28751453; PMCID: PMC5568816.
- Muñiz Pedrogo, David A., Sears, Cynthia L., Melia, Joanna M.P., October 2024. Colorectal cancer in inflammatory bowel disease: a review of the role of gut microbiota and bacterial biofilms in disease pathogenesis. J. Crohns Colitis 18 (10), 1713–1725. https://doi.org/10.1093/ecco-jcc/jjae061.
- Nass, R.M., Gaylinn, B.D., Rogol, A.D., Thorner, M.O., 2010. Ghrelin and growth hormone: story in reverse. Proc. Natl. Acad. Sci. U. S. A. 107 (19), 8501–8502. https://doi.org/10.1073/pnas.1002941107.
- Nyuyki, K.D., Cluny, N.L., Swain, M.G., Sharkey, K.A., Pittman, Q.J., 2018. Altered brain excitability and increased anxiety in mice with experimental colitis: consideration of hyperalgesia and sex differences. Front. Behav. Neurosci. 12, 58. https://doi.org/ 10.3389/fnbeh.2018.00058.
- Palandurkar, G.S., Kumar, S., 2023. Biofilm's impact on inflammatory bowel diseases. Cureus 15 (9), e45510. https://doi.org/10.7759/cureus.45510. Sep 18. PMID: 37868553; PMCID: PMC10585119.
- Peillex, C., Peiletier, M., 2020. The impact and toxicity of glyphosate and glyphosate based herbicides on health and immunity. J. Immunotoxicol. 17 (1), 163–174. https://doi.org/10.1080/1547691X.2020.1804492.
- Perry, R., Peng, L., Barry, N., et al., 2016. Acetate mediates a microbiome-brain-β-cell axis to promote metabolic syndrome. Nature 534, 213–217. https://doi.org/10.1038/nature18309.
- Pesticide Action Network International. (n.d.). Glyphosate. https://pan-international.org/wp-content/uploads/Glyphosate-monograph.pdf.
- Rahman, A., Rao, M.S., Khan, K.M., 2018. Intraventricular infusion of quinolinic acid impairs spatial learning and memory in young rats: a novel mechanism of leadinduced neurotoxicity. J. Neuroinflammation 15, 263. https://doi.org/10.1186/ s12974-018-1306-2.
- Rigottier-Gois, L., 2013. Dysbiosis in inflammatory bowel diseases: the oxygen hypothesis. ISME J. 7, 1256–1261. https://doi.org/10.1038/ismej.2013.80.
- Robertson, S.J., Lemire, P., Maughan, H., Goethel, A., Turpin, W., Bedrani, L., Guttman, D.S., Croitoru, K., Girardin, S.E., Philpott, D.J., 2019. Comparison of cohousing and littermate methods for microbiota standardization in mouse models. Cell Reports (Cambridge) 27 (6), 1910–1919 e2. https://doi.org/10.1016/j.
- Romano, S., Savva, G.M., Bedarf, J.R., Charles, I.G., Hildebrand, F., Narbad, A., 2021. Meta-analysis of the parkinson's disease gut microbiome suggests alterations linked to intestinal inflammation. NPJ Parkinson's Disease 7 (1), 27. https://doi.org/ 10.1038/s41531-021-00156-2
- Schaeffer, E., Kluge, A., Böttner, M., Zunke, F., Cossais, F., Berg, D., Arnold, P., 2020. Alpha synuclein connects the gut-brain axis in Parkinson's disease patients – A view on clinical aspects, cellular pathology and analytical methodology. Frontiers in Cell and Developmental Biology 8, 573696. https://doi.org/10.3389/fcell.2020.573696.
- Semchuk, K.M., Love, E.J., Lee, R.G., 1992. Parkinson's disease and exposure to agricultural work and pesticide chemicals. Neurology 42 (7), 1328. https://doi.org/ 10.1212/wnl.42.7.1328.
- Shen, Z., Zhang, M., Liu, Y., Ge, C., Lu, Y., Shen, H., Zhu, L., 2024. Prevalence of metabolic syndrome in patients with inflammatory bowel disease: A systematic review and meta-analysis. BMJ Open 14 (3), e074659. https://doi.org/10.1136/ https://doi.org/10.1136/
- Shi, M., Yue, Y., Ma, C., Dong, L., Chen, F., 2022. Pasteurized *Akkermansia muciniphila*Ameliorate the LPS-Induced Intestinal Barrier Dysfunction via Modulating AMPK
 and NF-κB through TLR2 in Caco-2 Cells. Nutrients 14 (4), 764. https://doi.org/
 10.3390/nu14040764. PMID: 35215413; PMCID: PMC8879293. Feb 11.
- Stępniowska, A., Tutaj, K., Juśkiewicz, J., Ognik, K., 2022 Mar. Effect of a high-fat diet and chromium on hormones level and Cr retention in rats. J Endocrinol Invest. 45 (3), 527–535. https://doi.org/10.1007/s40618-021-01677-3. Epub 2021 Sep 22. PMID: 34550535: PMCID: PMC8850218.
- Sun, Z., Lee-Sarwar, K., Kelly, R.S., Lasky-Su, J.A., Litonjua, A.A., Weiss, S.T., Liu, Y.Y., 2023 Apr. Revealing the importance of prenatal gut microbiome in offspring neurodevelopment in humans. EBioMedicine 90, 104491. https://doi.org/10.1016/j.ebiom.2023.104491. Epub 2023 Mar 1. PMID: 36868051; PMCID: PMC9996363.
- Taglialegna, A., 2024. Feeling the blues with parabacteroides. Nat. Rev. Microbiol. 22 (3), 120. https://doi.org/10.1038/s41579-024-01016-2.
- TriplePundit, 2016. Residue of herbicide glyphosate found in common breakfast foods. https://www.triplepundit.com/story/2016/residue-herbicide-glyphosate-found-common-breakfast-foods/26446.
- Tsai, J.P., 2017. The association of serum leptin levels with metabolic diseases. Ci ji yi xue za zhi =Tzu-chi medical journal 29 (4), 192–196. https://doi.org/10.4103/tcmj.tcmj 123 17.

- University of North Carolina at Chapel Hill. (2021, April 08). Mouse diet and feeding behavior. Retrieved July 3, 2024, from https://policies.unc.edu/TDClient/2833/Portal/KB/ArticleDet?ID=132199.
- Vainshelboim, I. (2015, March 25). Honey found to have high levels of Roundup herbicide glyphosate. Digital Journal. https://www.digitaljournal.com/life/hone y-found-to-have-high-levels-of-roundup-herbicide-glyphosate/article/426458. Digital Journal, 2015. Honey found to have high levels of Roundup herbicide glyphosate. March 25 https://www.digitaljournal.com/life/honey-found-to-have-high-levels-of-roundup-herbicide-glyphosate/article/426458.
- von Boyen, G.B., Schulte, N., Pflüger, C., et al., 2011. Distribution of enteric glia and GDNF during gut inflammation. BMC Gastroenterol. 11, 3. https://doi.org/10.1186/1471-230X-11-3
- Vuong, H.E., Pronovost, G.N., Williams, D.W., et al., 2020. The maternal microbiome modulates fetal neurodevelopment in mice. Nature 586, 281–286. https://doi.org/ 10.1038/s41586-020-2745-3.
- Wang, W., Chen, L., Zhou, R., Wang, X., Song, L., Huang, S., Wang, G., Xia, B., 2014. Increased proportions of bifidobacterium and the lactobacillus group and loss of butyrate-producing bacteria in inflammatory bowel disease. J. Clin. Microbiol. 52 (2), 398–406. https://doi.org/10.1128/JCM.01500-13.
- Ward, T., Larson, J.E., Meulemans, J., Hillmann, B., Lynch, J., Sidiropoulos, D.N., Knights, D., 2017. Bugbase Predicts Organism-level Microbiome Phenotypes. https://doi.org/10.1101/133462
- Waters, J.L., Ley, R.E., 2019. The human gut bacteria christensenellaceae are widespread, heritable, and associated with health. BMC Biol. 17 (1), 83. https://doi. org/10.1186/s12915-019-0699-4.
- Wu, Rongqian, Dong, Weifeng, Qiang, Xiaoling, Wang, Haichao, Blau, Steven A., Ravikumar, Thanjavur S., Wang, Ping, August 2009. Orexigenic hormone ghrelin ameliorates gut barrier dysfunction in sepsis in rats*. Crit. Care Med. 37 (8), 2421–2426. https://doi.org/10.1097/CCM.0b013e3181a557a2.